

Non-Hermitian skin modes induced by on-site dissipations and chiral tunneling effect

Yifei Yi^{1,2} and Zhesen Yang^{1,2*}

¹Beijing National Laboratory for Condensed Matter Physics,
and Institute of Physics, Chinese Academy of Sciences, Beijing 100190, China and

²University of Chinese Academy of Sciences, Beijing 100049, China

(Dated: August 22, 2022)

In this paper, we study the conditions under which on-site dissipations can induce non-Hermitian skin modes in non-Hermitian systems. When the origin Hermitian Hamiltonians have spinless time-reversal symmetry, it is impossible to have skin modes; on the other hand, if the Hermitian Hamiltonian has spinful time-reversal symmetry, skin modes can be induced by on-site dissipations under certain circumstance. As a concrete example, we employ the Rice-Mele model to illustrate our results. Furthermore, we predict that the skin modes can be detected by the chiral tunneling effect.

Introduction.—Non-Hermitian Hamiltonians [1–3], which describe the nonconservative phenomena [4], have been widely studied in many fields of physics, such as photonics [4–8], cold atoms [9–13], condensed matter systems [14–29] and open quantum systems [30, 31]. Recently, it has been shown that some non-Hermitian Hamiltonians can never be characterized by a Bloch Hamiltonian [31–59]. To be more precise, the open boundary spectra may collapse compared to the periodic boundary spectra, along with the emergence of non-Hermitian skin modes [32]. It has been shown that both phenomena can be well understood with the concept of generalized Brillouin zone (GBZ) [32–37], which is a generalization of Brillouin zone (BZ) defined in systems (Hermitian or non-Hermitian) with periodic boundaries to ones with open boundaries. When the GBZ coincides with the BZ, the open boundary spectra can be described by the Bloch Hamiltonian with no skin modes; and the conventional bulk-boundary correspondence still holds. On the other hand, if GBZ is distinct from BZ, then the open boundary spectra collapses, and skin modes along with the anomalous bulk-boundary correspondence emerge at the same time [32]. Inspired by the theoretical proposal, non-Hermitian skin modes have been observed experimentally in the classical wave systems recently [60–63]. Finding the condition of the emergence of these skin modes in quantum systems and investigating the corresponding novel physical response are interesting and challenging [64–95].

On-site dissipations are well-controlled non-Hermitian terms that can be realized experimentally in both classical and quantum systems [4–8, 96–101]. In contrast to the non-reciprocal terms, like $\sum_i (t\hat{a}_i^\dagger \hat{b}_i + 2t\hat{b}_i^\dagger \hat{a}_i)$, on-site dissipations, such as $\sum_i (i\gamma_a \hat{a}_i^\dagger \hat{a}_i + i\gamma_b \hat{b}_i^\dagger \hat{b}_i)$, do not favor any special hopping direction. Although it has been revealed that skin modes can be induced by on-site dissipations [13, 31, 62], the relationship between skin modes and on-site dissipations is still unclear.

In this paper, we show that if a Hermitian non-superconductivity system has spinless time-reversal symmetry (TRS), on-site dissipations will not induce non-

Hermitian skin modes. However, if the Hermitian system has spinful TRS, it is possible for the system to have skin modes depending on whether the system has inversion symmetry (IS) and the representation of it. As a concrete example, we use Rice-Mele model to illustrate our results. We also clarify the relationship between Hermitian and non-Hermitian symmetries. The novel physical response of skin modes is also investigated.

Non-Hermitian Hamiltonians with on-site dissipations.—We start from the following one-dimensional (1D) Hermitian Hamiltonian,

$$\hat{H} = \hat{H}_s + \hat{H}_b + \hat{H}_{s-b}. \quad (1)$$

Here $\hat{H}_s = \sum_{i,j} \sum_{\mu,\nu} t_{ij}^{\mu\nu} \hat{c}_{i\mu}^\dagger \hat{c}_{j\nu}$ is the system Hamiltonian we concerned, where i, j and μ, ν label lattice sites and band (or spin) indexes, respectively; $\hat{H}_b = \sum_{i,p_\mu,\mu} (\varepsilon_{p_\mu} - \mu_{p_\mu}) \hat{b}_{ip_\mu}^\dagger \hat{b}_{ip_\mu}$ comes from a free Fermion bath, where p_μ is the internal degrees of the bath; and $\hat{H}_{s-b} = \sum_{i,p_\mu,\mu} V_{p_\mu\mu} (\hat{c}_{i\mu}^\dagger \hat{b}_{ip_\mu} + \hat{b}_{ip_\mu}^\dagger \hat{c}_{i\mu})$ is the system-bath coupling term. We first focus on the periodic boundary condition. When the external bath degrees are integrated out, we can obtain the following Dyson equation of the retarded Green's function: $G_s^R(k, \omega) = [\omega - \mathcal{H}_s(k) - \Sigma_b^R(\omega)]^{-1}$, where $[\mathcal{H}_s(k)]_{\mu\nu} = \sum_{l_{\mu\nu}} t_{l_{\mu\nu}}^{\mu\nu} e^{ikl_{\mu\nu}}$ is the Bloch Hamiltonian of the system and the diagonal matrix $[\Sigma_b^R(\omega)]_{\mu\nu} = \delta_{\mu\nu} \sum_{p_\mu} |V_{p_\mu\mu}|^2 / (\omega - \varepsilon_{p_\mu} + \mu_{p_\mu} + i\eta)$ with $\eta = 0^+$ is the self-energy correction. The imaginary part of the self-energy correction is the spectral function of the external bath $[\Gamma(\omega)]_{\mu\nu} = \pi \delta_{\mu\nu} \sum_{p_\mu} |V_{p_\mu\mu}|^2 \delta(\omega - \varepsilon_{p_\mu} + \mu_{p_\mu})$. A simple treatment of the dissipation is to assume an uniform distribution of $[\Gamma(\omega)]_{\mu\nu}$ in the region $[-W, W]$ [102]. If $2W$ is much larger than the band width of the system we concerned, $\Gamma(\omega)$ can be approximated by a constant diagonal matrix $i\gamma\Gamma_0$, and the corresponding non-Hermitian effective Bloch Hamiltonian can be written as

$$\mathcal{H}_{s,eff}(k) = \mathcal{H}_s(k) - i\gamma\Gamma_0, \quad (2)$$

where γ is proportional to the density of states (DoS) of the external bath and the system-bath coupling strength,

TABLE I. Non-Hermitian symmetry ramifications. All the 1D Hermitian (non-Hermitian) symmetry groups can be generated by the symmetries listed in the first (second and fourth) row. If the Hermitian part of the Hamiltonian has one of the eight Hermitian symmetries listed in the first row, then the corresponding non-Hermitian symmetries, listed in the second and fourth rows, will be preserved for the overall non-Hermitian Hamiltonian, supposing that the on-site dissipation term Γ_0 is commutative or anti-commutative to the unitary representation of these Hermitian symmetries. The third and fifth rows represent the constraints these symmetries impose on the characteristic equation $f(\beta, E) = \det[E - \mathcal{H}_{s,eff}(\beta)]$, where $\beta = e^{ik}$ is extended to the entire complex plane in non-Hermitian systems.

	Hermitian	I	\mathcal{PT}	\mathcal{P}	\mathcal{T}	\mathcal{TC}	\mathcal{PC}	\mathcal{PTC}	\mathcal{C}
	Non-Hermitian	I	$\mathcal{P}\bar{\mathcal{T}}$	\mathcal{P}	$\bar{\mathcal{T}}$	$\mathcal{TC}, \bar{\mathcal{T}}\bar{\mathcal{C}}$	$\mathcal{P}\bar{\mathcal{C}}$	$\mathcal{PTC}, \mathcal{P}\bar{\mathcal{T}}\bar{\mathcal{C}}$	$\bar{\mathcal{C}}$
$[\Gamma_0, U_X] = 0$	$U_X^{-1}\mathcal{H}(k)U_X =$	$\mathcal{H}(k)$	$\mathcal{H}^t(k)$	$\mathcal{H}(-k)$	$\mathcal{H}^t(-k)$	$-\mathcal{H}^\dagger(k)$	$-\mathcal{H}^*(k)$	$-\mathcal{H}^\dagger(-k)$	$-\mathcal{H}^*(-k)$
	$f(\beta, E) =$	$f(\beta, E)$		$f(1/\beta, E)$		$f(1/\beta^*, -E^*)$		$f(\beta^*, -E^*)$	
	Non-Hermitian	$\mathcal{T}\bar{\mathcal{T}}, \mathcal{C}\bar{\mathcal{C}}$	\mathcal{PT}	$\mathcal{PT}\bar{\mathcal{T}}, \mathcal{PC}\bar{\mathcal{C}}$	\mathcal{T}	$\bar{\mathcal{T}}\mathcal{C}, \mathcal{T}\bar{\mathcal{C}}$	\mathcal{PC}	$\mathcal{P}\bar{\mathcal{T}}\mathcal{C}, \mathcal{PT}\bar{\mathcal{C}}$	\mathcal{C}
$\{\Gamma_0, U_X\} = 0$	$U_X^{-1}\mathcal{H}(k)U_X =$	$\mathcal{H}^\dagger(k)$	$\mathcal{H}^*(k)$	$\mathcal{H}^\dagger(-k)$	$\mathcal{H}^*(-k)$	$-\mathcal{H}(k)$	$-\mathcal{H}^t(k)$	$-\mathcal{H}(-k)$	$-\mathcal{H}^t(-k)$
	$f(\beta, E) =$	$f(1/\beta^*, E^*)$		$f(\beta^*, E^*)$		$f(\beta, -E)$		$f(1/\beta, -E)$	

and Γ_0 is a *diagonal matrix* satisfying $\Gamma_0 = \Gamma_0^* = \Gamma_0^t$. This kind of dissipation is dubbed as *on-site dissipation* in this paper. Searching for the conditions for the emergence of skin modes for this type of non-Hermitian Hamiltonian is the central topic of this paper.

Non-Hermitian symmetry and skin modes.—The main results of this paper can be summarized as follows. If the Hermitian Hamiltonian $\mathcal{H}_s(k)$ in Eq. 2 preserves TRS but breaks particle-hole symmetry (PHS) [103], then, (i) for the spinless case, it is impossible to have skin modes; (ii) for the spinful case, if the skin modes are to emerge, one of the following three conditions must be satisfied: (a) $\mathcal{H}_s(k)$ breaks IS; (b) $\mathcal{H}_s(k)$ preserves IS represented by \mathcal{P} , but anti-commutes with the on-site dissipation, namely, $\{\mathcal{P}, \Gamma_0\} = 0$; (c) $\mathcal{H}_s(k)$ preserves IS and $[\mathcal{P}, \Gamma_0] = [\mathcal{T}, \Gamma_0] = 0$, but $\{\mathcal{P}, \mathcal{T}\} = 0$ [103–105], where \mathcal{T} is the representation of TRS.

When $\gamma = 0$, Eq. 2 reduces to the Hermitian limit and all the 1D symmetry groups can be generated by the 8 symmetries listed in the first row of Table. I [106], where $\mathcal{T}, \mathcal{C}, \mathcal{P}$ represent TRS, PHS, and IS, respectively. However, when $\gamma \neq 0$, the symmetries will be ramified [71] due to $\mathcal{H}^\dagger \neq \mathcal{H}$ and all the 1D non-Hermitian symmetry groups can be generated by the 16 symmetries listed in the second and fifth rows of Table. I [106], where $\bar{\mathcal{T}}, \bar{\mathcal{C}}$ represent the anomalous time-reversal symmetry (TRS †) and anomalous particle-hole symmetry (PHS †), respectively. The symmetry constraints to the Bloch Hamiltonian are shown in the third and sixth rows of Table. I. For example, systems with TRS satisfy $U_{\mathcal{T}}\mathcal{H}^*(k)U_{\mathcal{T}}^{-1} = \mathcal{H}(-k)$ and systems with TRS † satisfy $U_{\bar{\mathcal{T}}}\mathcal{H}^t(k)U_{\bar{\mathcal{T}}}^{-1} = \mathcal{H}(-k)$ [71].

As mentioned earlier, the Hermitian Hamiltonian $\mathcal{H}_s(k)$ in Eq. 2 is assumed to preserve TRS (represented by $\mathcal{T} = U_{\mathcal{T}}\mathcal{K}^*$, where \mathcal{K}^* represent the complex conjugate operator), and it is obvious that TRS and TRS † (represented by $\bar{\mathcal{T}} = U_{\bar{\mathcal{T}}}\mathcal{K}^t$, where \mathcal{K}^t represent the transpose operator) are equivalent in Hermitian cases. Therefore,

it can be easily deduced that if the on-site dissipation Γ_0 is commutative to $U_{\mathcal{T}}$, namely $[\Gamma_0, U_{\mathcal{T}}] = 0$, TRS is broken but TRS † is preserved for the overall non-Hermitian Hamiltonian $\mathcal{H}_{s,eff}$. On the other hand, if $\{\Gamma_0, U_{\mathcal{T}}\} = 0$, TRS † is broken but TRS is preserved. In fact, each of the non-Hermitian symmetry has a Hermitian origin and obeys the similar rule, as shown in Table. I [106]. The symmetry ramification depends on the commutation relation.

We now show the main result mentioned above. Assume that the Hermitian Hamiltonian $\mathcal{H}_s(k)$ breaks PHS but preserves TRS, then, the Hamiltonian can be classified by the following ten Hermitian symmetry groups [106]: $G_{\mathcal{T}_\pm}, G_{\mathcal{T}_\pm, (\mathcal{PT})_\pm}, G_{\mathcal{T}_\pm, (\mathcal{PC})_\pm}$, where the lower index X_\pm represents the *group generators* with $U_X U_X^* = \pm 1$. With the existence of on-site dissipation, besides the above groups, the following 26 non-Hermitian symmetry groups can be ramified [106] $G_{\bar{\mathcal{T}}_\pm}, G_{\bar{\mathcal{T}}_\pm, (\mathcal{P}\bar{\mathcal{T}})_\pm}, G_{\bar{\mathcal{T}}_\pm, (\mathcal{PT})_\pm}, G_{\bar{\mathcal{T}}_\pm, (\mathcal{P}\bar{\mathcal{T}})_\pm}, G_{\mathcal{T}_\pm, (\mathcal{P}\bar{\mathcal{C}})_\pm}, G_{\bar{\mathcal{T}}_\pm, (\mathcal{PC})_\pm}, G_{\bar{\mathcal{T}}_\pm, (\mathcal{P}\bar{\mathcal{C}})_\pm}$.

Next, we will show how these symmetries constrain the emergence of skin modes. We first need to derive the constraints these symmetries impose on the characteristic equation of the non-Bloch Hamiltonian [32–37]: $f(\beta, E) = \det[E - \mathcal{H}_{s,eff}(\beta)]$, where $\beta = e^{ik}$. The result is shown in the fourth and seventh rows of Table. I [106]. Combining these result with the GBZ condition shown in Table. II [32, 35–37, 107], one can find that the GBZ is constrained to be the unit circle when some specific symmetries exist [71]. For example, if a N -band system only has IS (\mathcal{P}) or spinless TRS † ($\bar{\mathcal{T}}_+$), then, according to Table. I, we have $f(\beta, E) = f(1/\beta, E)$, which means f can be expressed as $f(\beta, E) = \sum_{n=0}^p \sum_{m=0}^N c_{nm}(\beta^n + 1/\beta^n)E^m$. Therefore, if β_p is a solution of $f(\beta, E_0) = 0$, then $\beta_{p+1} = 1/\beta_p$ is also a solution with the same E_0 . On the other hand, the GBZ condition shown in Table. II requires $|\beta_p| = |\beta_{p+1}|$ [32, 35–37], thus, we can conclude, $|\beta_p| = |\beta_{p+1}| = 1$. This means the skin modes are absent

TABLE II. GBZ condition for the non-Hermitian symmetry generators [107].

$\bar{\mathcal{T}}_-$	$E \in \mathbb{C}$	$ \beta_{p-1} = \beta_p \ \& \ \beta_{p+1} = \beta_{p+2} $
$(\mathcal{PT})_-$	$E \in \mathbb{R}$	
$(\mathcal{PC})_-$	$iE \in \mathbb{R}$	
$(\mathcal{PT})_-$	$E \in \mathbb{C}$	$ \beta_{p-1} = \beta_p = \beta_{p+1} = \beta_{p+2} $
\mathcal{T}_-	$E \in \mathbb{R}$	
$\bar{\mathcal{C}}_-$	$iE \in \mathbb{R}$	
Others	$E \in \mathbb{C}$	

and there is no open boundary spectra collapse. However, if the system has spinful TRS^\dagger ($\bar{\mathcal{T}}_-$), the open boundary spectra will be of double degeneracy corresponding to two distinct spin bands, and for each band, the GBZ condition must be satisfied separately, therefore, the overall GBZ condition will be changed from $|\beta_p| = |\beta_{p+1}|$ to $|\beta_{p-1}| = |\beta_p| \ \& \ |\beta_{p+1}| = |\beta_{p+2}|$. As a result, the absence of skin modes is no longer obliged in such systems.

Follow the same steps, one can find that for all the non-Hermitian symmetry groups listed above, skin modes are absent when G contains $\bar{\mathcal{T}}_+$, or \mathcal{P} . An exceptional case is $G_{\bar{\mathcal{T}}_-, (\mathcal{PT})_+}$, where the skin modes emerge with the presence of IS. We emphasize that the above results are quite general and independent of the choice of non-Hermitian models. The complete proof and numerical verification can be found in the Supplemental Materials [106]. This result is consistent with the main result listed above. To show this, consider a spinless *Hermitian* system with $\text{TRS} \mathcal{T}_+ = \mathcal{K}^*$, it is obvious $[U_{\mathcal{T}_+}, \Gamma_0] = 0$. This implies the non-Hermitian Hamiltonian must preserve $\bar{\mathcal{T}}_+$. Thus it is impossible to have skin modes. This is the main result (i) discussed above. For the spinful case with $\mathcal{T}_- = U_{\mathcal{T}_-} \mathcal{K}^*$, if $\mathcal{H}_s(k)$ has $\mathcal{P} = U_{\mathcal{P}}$ and commutative to the on-site dissipation $[U_{\mathcal{P}}, \Gamma_0] = 0$, the non-Hermitian Hamiltonian must preserve IS. This forbids the emergence of skin modes in general. For the exceptional case, the existence of $\bar{\mathcal{T}}_-$ and $(\mathcal{PT})_+$ symmetries imply the Hermitian Hamiltonian $\mathcal{H}_s(k)$ must preserve \mathcal{T}_- and $(\mathcal{PT})_+$ symmetries, which implies the anti-commutation relation of the following two Hermitian symmetries $\{\mathcal{P}, \mathcal{T}\} = 0$ [106]. The above result is equivalent to the main result (ii).

Example.—In order to verify our results, we use Rice-Mele model as an example with the following Bloch Hamiltonian

$$\mathcal{H}_{\text{RM}}(k) = (t_1 + t_2 \cos k)\sigma_x + t_2 \sin k\sigma_y + \mu\sigma_z, \quad (3)$$

which preserves $\mathcal{T}_+ = \mathcal{K}^*$, $(\mathcal{PC})_- = \sigma_y \mathcal{K}^t$, $\mathcal{PCT} = \sigma_y \mathcal{K}^\dagger$. In order to have skin modes, we can either break TRS or add spin-orbit coupling. For the first case, TRS can be broken by adding π -flux as shown in Fig. 1 (a) with the

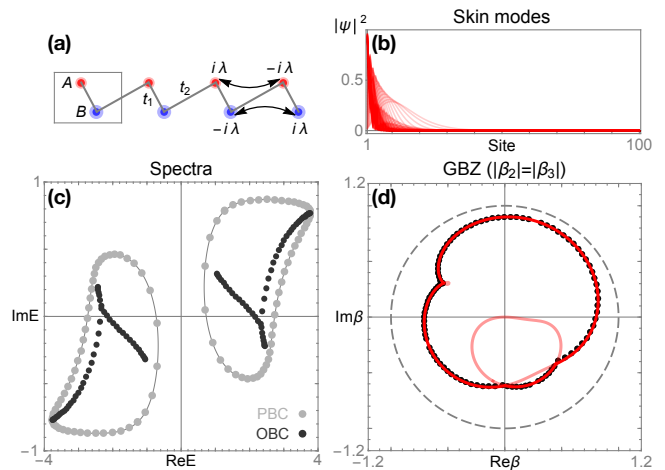


FIG. 1. The spinless model Eq. 4 possessed of skin modes. (a) shows the schematic diagram of the *Hermitian* part, namely $\mathcal{H}_{\text{RM}}(k) + \lambda \sin k\sigma_z$. (b) shows all the eigenstates (skin modes) of the model with $t_1 = \lambda = 2, t_2 = \mu = \gamma = 1$. In addition, (c) shows the spectra with open/periodic boundary condition and (d) shows the numerical GBZ (black points) and auxiliary GBZ [37] (red lines) of the system

following Bloch Hamiltonian

$$\mathcal{H}_{\text{spinless}}(k) = \mathcal{H}_{\text{RM}}(k) + \lambda \sin k\sigma_z + i\gamma\sigma_z. \quad (4)$$

It is easy to verify that only $(\mathcal{PC})_-$ symmetry is preserved in Eq. 4. According to the GBZ condition ($|\beta_p| = |\beta_{p+1}|$) shown in Table. II and the symmetry constraint ($f(\beta, E) = f(\beta, -E)$) shown in Table. I, we can deduce that (i) the spectra are formed by pairs $(E, -E)$; (ii) the roots of the characteristic equation satisfy $\beta(E) = \beta(-E)$, which means the sub-GBZs [37] for the E and $-E$ bands are the same. As shown in Fig. 1 (b), all the wavefunctions of Eq. 4 with $t_1 = \lambda = 2, t_2 = \mu = \gamma = 1$ and $N = 100$ are plotted. One can notice that all the wavefunctions are localized at the left boundary. The existence of skin modes is also equivalent to the discrepancy between periodic and open boundary spectra shown in Fig. 1 (c). The corresponding numerical calculation of GBZ (black points) and auxiliary GBZ [37] (red lines) are shown in Fig. 1 (d), which are both inside the unit circle (gray dashed lines). In the Supplemental Materials, we show that regardless the value of μ , the skin modes always exist when $\lambda t_1 t_2 \neq 0$ [106]. This means the on-site dissipations can also induce skin modes in the Su-Schrieffer-Heeger model when TRS is broken.

For the spinful case, since the Rice-Mele model breaks IS, on-site dissipation can induce skin modes if we add spin-orbit coupling. Therefore, the following Bloch Hamiltonian with intrinsic and shortest ranged Rashiba spin-orbit coupling is studied

$$\begin{aligned} \mathcal{H}_{\text{spinful}}(k) &= \mathcal{H}_{\text{RM}}(k)s_0 + \mathcal{H}_{\text{soc}}(k) + i\gamma\sigma_z s_0, \\ \mathcal{H}_{\text{soc}}(k) &= \lambda_I \sin k\sigma_z s_z - \lambda_R \sigma_y (s_x - \sqrt{3}s_y)/2, \end{aligned} \quad (5)$$

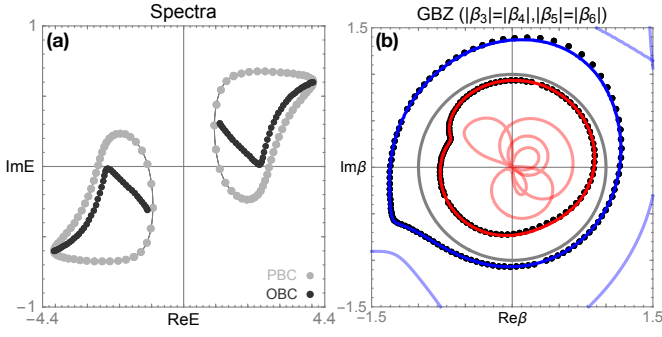


FIG. 2. The spectra and GBZ of the spinful model Eq. 5 with $t_1 = \lambda_I = 2, t_2 = \mu = \lambda_R = \gamma = 1$. (a) shows the spectra of the system with periodic/open boundary conditions. The discrepancy indicates the emergence of skin modes. (b) shows the corresponding auxiliary GBZ (solid lines) and numerical calculation of GBZ (Block points). Notice that the GBZ condition for the system with spinful TRS † is $|\beta_{p-1}| = |\beta_p|$ & $|\beta_{p+1}| = |\beta_{p+2}|$, and in this case $p = 4$.

where s is the spin Pauli matrix. Under the action of spinful TRS † , $|\beta, E, \uparrow\rangle$ maps to $|\beta, E, \downarrow\rangle$. Therefore, a left localized eigenstate with $|\beta| < 1$ will be mapped to the right with $|\beta| > 1$. These skin modes are dubbed as Z_2 skin modes [38] and protected by TRS † . Indeed, according to the GBZ condition $|\beta_{p-1}| = |\beta_p| = 1/r_0$ for one spin band, and $|\beta_{p+1}| = |\beta_{p+2}| = r_0$ for the other, the absence of IS implies there is no guarantee of $1/r_0 = r_0$. Therefore, skin modes can emerge. This can be checked by the comparison of open/periodic boundary spectra and the corresponding GBZ shown in Fig. 2 with the following parameters $t_1 = \lambda_I = 2, t_2 = \mu = \lambda_R = \gamma = 1$. As shown in (b), the GBZ for one spin band (the red lines containing the black points) is larger than 1, and the other (the blue lines containing the black points) is smaller than 1. In the Supplemental Materials, we provide a Mathematica code to calculate the corresponding GBZ and auxiliary GBZ [106].

Chiral tunneling effect.—We now investigate the novel physical response induced by skin modes. It turns out that (i) the boundary localized skin modes *does not* imply the large local DoSs (LDoS) at the boundary, which means the skin modes can not be detected directly by the measurement of LDoS; (ii) the existence of skin modes can be detected by chiral tunneling effect. When the system has skin modes, the corresponding eigenstates $|\psi_{n,\beta}^R\rangle$ of $H_{s,eff}$ is a superposition of several non-Bloch waves with $H_{s,eff}|\psi_{n,\beta}^R\rangle = E_n|\psi_{n,\beta}^R\rangle$. Here β in $|\psi_{n,\beta}^R\rangle$ is used to emphasize it maybe skin mode. Using the bi-orthogonal basis, $H_{s,eff}^\dagger|\psi_{n,\beta}^L\rangle = E_n^*|\psi_{n,\beta}^L\rangle$ and $\langle\psi_{m,\beta}^L|\psi_{n,\beta}^R\rangle = \delta_{mn}$, the retarded Green's function and time evolution operator can be expressed as

$$G_s(\omega) = \sum_n \frac{|\psi_{n,\beta}^R\rangle\langle\psi_{n,\beta}^L|}{\omega - E_n}, U_s(t) = \sum_n e^{-iE_n t} |\psi_{n,\beta}^R\rangle\langle\psi_{n,\beta}^L|. \quad (6)$$

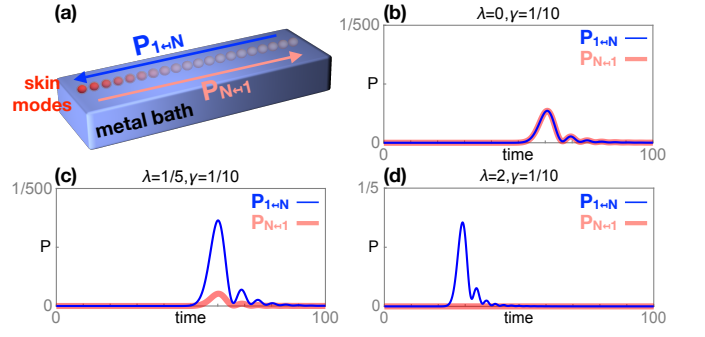


FIG. 3. Chiral tunneling effect induced by the skin modes. (a) shows the setup and the corresponding left localized skin modes. (b)-(d) show the skin modes localization (left-moving) direction is favored when we increase λ in $H_{\text{spinless}} - i\gamma\sigma_0$ with $t_1 = 2, t_2 = \mu = 1, \gamma = 1/10$.

In the Supplemental Materials, we show that $|\psi_{n,\beta}^R\rangle = U(r_n)|\psi_{n,k}^R\rangle$ and $\langle\psi_{n,\beta}^L| = \langle\psi_{n,k}^L|U(1/r_n)$, where $U(r_n) = \text{diag}[r_n, r_n^2, \dots, r_n^N]$, $r_n = |\beta_n|$ which indicates the localization length of the skin modes, and $|\psi_{n,k}^R\rangle$ and $\langle\psi_{n,k}^L|$ are the superposition of conventional Bloch waves satisfying $\langle\psi_{n,k}^L|\psi_{n,k}^R\rangle = 1$ [106]. Therefore, the real space correlation functions and propagators between sites i and f become

$$\begin{aligned} \langle f|G_s^R(\omega)|i\rangle &= \sum_n r_n^{f-i} \frac{\langle f|\psi_{n,k}^R\rangle\langle\psi_{n,k}^L|i\rangle}{\omega - E_n}, \\ \langle f|U_s(t)|i\rangle &= \sum_n r_n^{f-i} e^{-iE_n t} \langle f|\psi_{n,k}^R\rangle\langle\psi_{n,k}^L|i\rangle. \end{aligned} \quad (7)$$

When $f = i$, $\nu_i(\omega) := -\text{Im}[\langle i|G_s(\omega)|i\rangle]/\pi$ defines the LDoS at site i , which is irrelevant to the localization length of skin modes (r_n). This means the local DoS do not carry the information of skin modes. However, as shown in Fig. 3 (a), if we focus on the probability of quantum tunneling from one end to the other, there is an asymmetry for different tunneling directions, that is, $P_{N\leftarrow 1}(t) = |\langle N|U(t)|1\rangle|^2 \propto r_n^{N-1}$ and $P_{1\leftarrow N}(t) = |\langle 1|U(t)|N\rangle|^2 \propto r_n^{1-N}$, when $r_n \neq 1$ for all n [108]. This is the chiral tunneling effect induced by skin modes. As shown in Fig. 3 (b)-(d), we plot $P_{N\leftarrow 1}(t)$ and $P_{1\leftarrow N}(t)$ of $H_{\text{spinless}} - i\gamma\sigma_0$ with $t_1 = 2, t_2 = \mu = 1, \gamma = 1/10, N = 100$ for different values of λ . When λ increase from zero to a nonzero value, skin modes emerge, in the meantime, $P_{1\leftarrow N}(t)$ increase and $P_{N\leftarrow 1}(t)$ decrease. This means tunneling along the direction in which the skin modes localize is favored. We noted that the chiral tunneling effect in our model can be experimental controlled by tuning of the external magnetic field we applied, which may be useful in the electronics studies.

Conclusion.—In summary, our results provide a new approach to realize and control skin modes by tuning the Hermitian Hamiltonian. Based on our results, for the non-superconductivity system with TRS, the simplest way to induce skin modes is to break TRS (or IS)

and add on-site dissipations. On the theoretical side, our standard Green's function method paves the way to study the novel physical response induced by non-Hermitian skin modes. On the experimental side, we expect our models and the prediction of chiral tunneling effect can be realized and observed in variety physical systems, ranging from condensed matter, cold atom to photonical systems.

Z. Yang thanks to the valuable discussion with Kai Zhang, Jiangping Hu, Andri Bernevig, Chen Fang, Ching-Kai Chiu, Dong E Liu, Haiping Hu, Chunhui Liu, Shenshan Qin and CongCong Le. The work is supported by the Ministry of Science and Technology of China 973 program (No. 2017YFA0303100), National Science Foundation of China (Grant No. NSFC-11888101, 1190020, 11534014, 11334012), and the Strategic Priority Research Program of CAS (Grant No.XDB07000000).

* Corresponding author: yangzs@iphy.ac.cn

- [1] C. M. Bender, *Rep. Prog. Phys.* **70**, 947 (2007).
- [2] I. Rotter, *Journal of Physics A: Mathematical and Theoretical* **42**, 153001 (2009).
- [3] N. Moiseyev, *Non-Hermitian Quantum Mechanics* (Cambridge University Press, 2011).
- [4] M.-A. Miri and A. Alù, *Science* **363**, eaar7709 (2019).
- [5] L. Feng, R. El-Ganainy, and L. Ge, *Nat. Photonics* **11**, 752 (2017).
- [6] R. El-Ganainy, K. G. Makris, M. Khajavikhan, Z. H. Musslimani, S. Rotter, and D. N. Christodoulides, *Nat. Phys.* **14**, 11 (2018).
- [7] Ş. K. Özdemir, S. Rotter, F. Nori, and L. Yang, *Nat. Mater.* **18**, 783 (2019).
- [8] T. Ozawa, H. M. Price, A. Amo, N. Goldman, M. Hafezi, L. Lu, M. C. Rechtsman, D. Schuster, J. Simon, O. Zilberberg, and I. Carusotto, *Rev. Mod. Phys.* **91**, 015006 (2019).
- [9] Y. Xu, S.-T. Wang, and L.-M. Duan, *Phys. Rev. Lett.* **118**, 045701 (2017).
- [10] M. Nakagawa, N. Kawakami, and M. Ueda, *Phys. Rev. Lett.* **121**, 203001 (2018).
- [11] K. Yamamoto, M. Nakagawa, K. Adachi, K. Takasan, M. Ueda, and N. Kawakami, *Phys. Rev. Lett.* **123**, 123601 (2019).
- [12] L. Pan, X. Chen, Y. Chen, and H. Zhai, arXiv e-prints, arXiv:1909.12516 (2019), [arXiv:1909.12516](https://arxiv.org/abs/1909.12516) [cond-mat.quant-gas].
- [13] L. Li, C. H. Lee, and J. Gong, arXiv e-prints, arXiv:1910.03229 (2019), [arXiv:1910.03229](https://arxiv.org/abs/1910.03229) [cond-mat.mes-hall].
- [14] V. M. Martinez Alvarez, J. E. Barrios Vargas, M. Berdakin, and L. E. F. Foa Torres, *Eur. Phys. J. Spec. Top.* **227**, 1295 (2018).
- [15] L. E. F. F. Torres, *Journal of Physics: Materials* **3**, 014002 (2019).
- [16] A. Ghatak and T. Das, *J. Phys.: Condens. Matter* **31**, 263001 (2019).
- [17] E. J. Bergholtz, J. C. Budich, and F. K. Kunst, arXiv e-prints, arXiv:1912.10048 (2019), [arXiv:1912.10048](https://arxiv.org/abs/1912.10048) [cond-mat.mes-hall].
- [18] N. Hatano and D. R. Nelson, *Phys. Rev. Lett.* **77**, 570 (1996).
- [19] M. S. Rudner and L. S. Levitov, *Phys. Rev. Lett.* **102**, 065703 (2009).
- [20] V. Kozii and L. Fu, arXiv e-prints, arXiv:1708.05841 (2017), [arXiv:1708.05841](https://arxiv.org/abs/1708.05841) [cond-mat.mes-hall].
- [21] M. Papaj, H. Isobe, and L. Fu, *Phys. Rev. B* **99**, 201107 (2019).
- [22] H. Shen and L. Fu, *Phys. Rev. Lett.* **121**, 026403 (2018).
- [23] T. Yoshida, R. Peters, and N. Kawakami, *Phys. Rev. B* **98**, 035141 (2018).
- [24] Y. Chen and H. Zhai, *Phys. Rev. B* **98**, 245130 (2018).
- [25] K. Moors, A. A. Zyuzin, A. Y. Zyuzin, R. P. Tiwari, and T. L. Schmidt, *Phys. Rev. B* **99**, 041116 (2019).
- [26] N. Okuma and M. Sato, *Phys. Rev. Lett.* **123**, 097701 (2019).
- [27] E. Lee, H. Lee, and B.-J. Yang, arXiv e-prints, arXiv:1912.05825 (2019), [arXiv:1912.05825](https://arxiv.org/abs/1912.05825) [cond-mat.mes-hall].
- [28] T. Yoshida, T. Mizoguchi, and Y. Hatsugai, arXiv e-prints, arXiv:1912.12022 (2019), [arXiv:1912.12022](https://arxiv.org/abs/1912.12022) [cond-mat.mes-hall].
- [29] M. Luo, arXiv e-prints, arXiv:2001.00697 (2020), [arXiv:2001.00697](https://arxiv.org/abs/2001.00697) [cond-mat.str-el].
- [30] S. Lieu, M. McGinley, and N. R. Cooper, *Phys. Rev. Lett.* **124**, 040401 (2020).
- [31] F. Song, S. Yao, and Z. Wang, *Phys. Rev. Lett.* **123**, 170401 (2019).
- [32] S. Yao and Z. Wang, *Phys. Rev. Lett.* **121**, 086803 (2018).
- [33] S. Yao, F. Song, and Z. Wang, *Phys. Rev. Lett.* **121**, 136802 (2018).
- [34] F. Song, S. Yao, and Z. Wang, *Phys. Rev. Lett.* **123**, 246801 (2019).
- [35] K. Yokomizo and S. Murakami, *Phys. Rev. Lett.* **123**, 066404 (2019).
- [36] K. Zhang, Z. Yang, and C. Fang, [arXiv:1910.01131](https://arxiv.org/abs/1910.01131).
- [37] Z. Yang, K. Zhang, C. Fang, and J. Hu, arXiv e-prints, arXiv:1912.05499 (2019), [arXiv:1912.05499](https://arxiv.org/abs/1912.05499) [cond-mat.mes-hall].
- [38] N. Okuma, K. Kawabata, K. Shiozaki, and M. Sato, [arXiv:1910.02878](https://arxiv.org/abs/1910.02878).
- [39] Y. Xiong, *J. Phys. Commun.* **2**, 035043 (2018).
- [40] F. K. Kunst, E. Edvardsson, J. C. Budich, and E. J. Bergholtz, *Phys. Rev. Lett.* **121**, 026808 (2018).
- [41] V. M. Martinez Alvarez, J. E. Barrios Vargas, and L. E. F. Foa Torres, *Phys. Rev. B* **97**, 121401 (2018).
- [42] C. H. Lee and R. Thomale, *Phys. Rev. B* **99**, 201103 (2019).
- [43] C. H. Lee, L. Li, R. Thomale, and J. Gong, arXiv e-prints, arXiv:1912.06974 (2019), [arXiv:1912.06974](https://arxiv.org/abs/1912.06974) [cond-mat.mes-hall].
- [44] S. Longhi, *Phys. Rev. Research* **1**, 023013 (2019).
- [45] L. Jin and Z. Song, *Phys. Rev. B* **99**, 081103 (2019).
- [46] T. Liu, Y.-R. Zhang, Q. Ai, Z. Gong, K. Kawabata, M. Ueda, and F. Nori, *Phys. Rev. Lett.* **122**, 076801 (2019).
- [47] C. H. Lee, L. Li, and J. Gong, *Phys. Rev. Lett.* **123**, 016805 (2019).
- [48] L. Herviou, J. H. Bardarson, and N. Regnault, *Phys. Rev. A* **99**, 052118 (2019).
- [49] R. Chen, C.-Z. Chen, B. Zhou, and D.-H. Xu, *Phys. Rev. B* **99**, 155431 (2019).
- [50] H. Jiang, L.-J. Lang, C. Yang, S.-L. Zhu, and S. Chen,

- Phys. Rev. B* **100**, 054301 (2019).
- [51] H.-G. Zirnstein, G. Refael, and B. Rosenow, [arXiv:1901.11241](#).
- [52] D. S. Borgnia, A. J. Kruchkov, and R.-J. Slager, *Phys. Rev. Lett.* **124**, 056802 (2020).
- [53] T.-S. Deng and W. Yi, *Phys. Rev. B* **100**, 035102 (2019).
- [54] X.-W. Luo and C. Zhang, *Phys. Rev. Lett.* **123**, 073601 (2019).
- [55] W. Brzezicki and T. Hyart, *Phys. Rev. B* **100**, 161105 (2019).
- [56] K.-I. Imura and Y. Takane, *Phys. Rev. B* **100**, 165430 (2019).
- [57] S. Longhi, [arXiv:1909.06211](#).
- [58] X.-R. Wang, C.-X. Guo, and S.-P. Kou, [arXiv e-prints](#), [arXiv:1912.04024](#) (2019), [arXiv:1912.04024 \[cond-mat.str-el\]](#).
- [59] R. Koch and J. C. Budich, [arXiv e-prints](#), [arXiv:1912.07687](#) (2019), [arXiv:1912.07687 \[cond-mat.mes-hall\]](#).
- [60] A. Ghatak, M. Brandenbourger, J. van Wezel, and C. Coulais, [arXiv e-prints](#), [arXiv:1907.11619](#) (2019), [arXiv:1907.11619 \[cond-mat.mes-hall\]](#).
- [61] T. Helbig, T. Hofmann, S. Imhof, M. Abdelghany, T. Kiessling, L. W. Molenkamp, C. H. Lee, A. Szameit, M. Greiter, and R. Thomale, [arXiv e-prints](#), [arXiv:1907.11562](#) (2019), [arXiv:1907.11562 \[cond-mat.mes-hall\]](#).
- [62] L. Xiao, T. Deng, K. Wang, G. Zhu, Z. Wang, W. Yi, and P. Xue, “Observation of non-hermitian bulk-boundary correspondence in quantum dynamics,” (2019), [arXiv:1907.12566](#).
- [63] T. Hofmann, T. Helbig, F. Schindler, N. Salgo, M. Brzezińska, M. Greiter, T. Kiessling, D. Wolf, A. Vollhardt, A. Kabaši, C. H. Lee, A. Bilušić, R. Thomale, and T. Neupert, [arXiv e-prints](#), [arXiv:1908.02759](#) (2019), [arXiv:1908.02759 \[cond-mat.mes-hall\]](#).
- [64] T. E. Lee, *Phys. Rev. Lett.* **116**, 133903 (2016).
- [65] D. Leykam, K. Y. Bliokh, C. Huang, Y. D. Chong, and F. Nori, *Phys. Rev. Lett.* **118**, 040401 (2017).
- [66] H. Shen, B. Zhen, and L. Fu, *Phys. Rev. Lett.* **120**, 146402 (2018).
- [67] S. Lieu, *Phys. Rev. B* **97**, 045106 (2018).
- [68] C. Yin, H. Jiang, L. Li, R. Lü, and S. Chen, *Phys. Rev. A* **97**, 052115 (2018).
- [69] Z. Gong, Y. Ashida, K. Kawabata, K. Takasan, S. Higashikawa, and M. Ueda, *Phys. Rev. X* **8**, 031079 (2018).
- [70] K. Kawabata, S. Higashikawa, Z. Gong, Y. Ashida, and M. Ueda, *Nature Communications* **10**, 297 (2019).
- [71] K. Kawabata, K. Shiozaki, M. Ueda, and M. Sato, *Phys. Rev. X* **9**, 041015 (2019).
- [72] S. Lieu, *Phys. Rev. B* **98**, 115135 (2018).
- [73] C.-H. Liu, H. Jiang, and S. Chen, *Phys. Rev. B* **99**, 125103 (2019).
- [74] H. Zhou and J. Y. Lee, *Phys. Rev. B* **99**, 235112 (2019).
- [75] J. Y. Lee, J. Ahn, H. Zhou, and A. Vishwanath, *Phys. Rev. Lett.* **123**, 206404 (2019).
- [76] H. Zhou, C. Peng, Y. Yoon, C. W. Hsu, K. A. Nelson, L. Fu, J. D. Joannopoulos, M. Soljačić, and B. Zhen, *Science* **359**, 1009 (2018), <https://science.sciencemag.org/content/359/6379/1009.full.pdf>.
- [77] A. Cerjan, S. Huang, M. Wang, K. P. Chen, Y. Chong, and M. C. Rechtsman, *Nature Photonics* **13**, 623 (2019).
- [78] X. Zhang, K. Ding, X. Zhou, J. Xu, and D. Jin, *Phys. Rev. Lett.* **123**, 237202 (2019).
- [79] J. Carlström and E. J. Bergholtz, *Phys. Rev. A* **98**, 042114 (2018).
- [80] Z. Yang and J. Hu, *Phys. Rev. B* **99**, 081102 (2019).
- [81] J. C. Budich, J. Carlström, F. K. Kunst, and E. J. Bergholtz, *Phys. Rev. B* **99**, 041406 (2019).
- [82] K. Kawabata, T. Bessho, and M. Sato, *Phys. Rev. Lett.* **123**, 066405 (2019).
- [83] Z. Yang, C.-K. Chiu, C. Fang, and J. Hu, [arXiv e-prints](#), [arXiv:1905.00210](#) (2019), [arXiv:1905.00210 \[cond-mat.mes-hall\]](#).
- [84] Z. Yang, A. P. Schnyder, J. Hu, and C.-K. Chiu, [arXiv e-prints](#), [arXiv:1912.02788](#) (2019), [arXiv:1912.02788 \[cond-mat.mes-hall\]](#).
- [85] X.-Q. Sun, C. C. Wojcik, S. Fan, and T. Bzdušek, [arXiv e-prints](#), [arXiv:1905.04338](#) (2019), [arXiv:1905.04338 \[cond-mat.mes-hall\]](#).
- [86] C. C. Wojcik, X.-Q. Sun, T. Bzdušek, and S. Fan, [arXiv e-prints](#), [arXiv:1911.12748](#) (2019), [arXiv:1911.12748 \[math-ph\]](#).
- [87] S. Longhi, *Phys. Rev. Lett.* **122**, 237601 (2019).
- [88] T. Biesenthal, M. Kremer, M. Heinrich, and A. Szameit, *Phys. Rev. Lett.* **123**, 183601 (2019).
- [89] B. Höckendorf, A. Alvermann, and H. Fehske, *Phys. Rev. Lett.* **123**, 190403 (2019).
- [90] H. Jiang, C. Yang, and S. Chen, *Phys. Rev. A* **98**, 052116 (2018).
- [91] F. K. Kunst and V. Dwivedi, *Phys. Rev. B* **99**, 245116 (2019).
- [92] X.-X. Zhang and M. Franz, *Phys. Rev. Lett.* **124**, 046401 (2020).
- [93] L. Li, C. H. Lee, and J. Gong, *Phys. Rev. B* **100**, 075403 (2019).
- [94] J. Hou, Y.-J. Wu, and C. Zhang, [arXiv e-prints](#), [arXiv:1906.03988](#) (2019), [arXiv:1906.03988 \[cond-mat.mes-hall\]](#).
- [95] S. Longhi, *Phys. Rev. Lett.* **124**, 066602 (2020).
- [96] R. Bouganne, M. Bosch Aguilera, A. Ghermaoui, J. Beugnon, and F. Gerbier, *Nature Physics* **16**, 21 (2020).
- [97] T. Tomita, S. Nakajima, I. Danshita, Y. Takasu, and Y. Takahashi, *Science Advances* **3** (2017), 10.1126/sciadv.1701513, <https://advances.sciencemag.org/content/3/12/e1701513.full.pdf>.
- [98] T. Tomita, S. Nakajima, Y. Takasu, and Y. Takahashi, *Phys. Rev. A* **99**, 031601 (2019).
- [99] J. Li, A. K. Harter, J. Liu, L. de Melo, Y. N. Joglekar, and L. Luo, *Nature Communications* **10**, 855 (2019).
- [100] N. Syassen, D. M. Bauer, M. Lettner, T. Volz, D. Dietze, J. J. García-Ripoll, J. I. Cirac, G. Rempe, and S. Dürr, *Science* **320**, 1329 (2008), <https://science.sciencemag.org/content/320/5881/1329.full.pdf>.
- [101] G. Barontini, R. Labouvie, F. Stubenrauch, A. Vogler, V. Guarrera, and H. Ott, *Phys. Rev. Lett.* **110**, 035302 (2013).
- [102] H. Aoki, N. Tsuji, M. Eckstein, M. Kollar, T. Oka, and P. Werner, *Rev. Mod. Phys.* **86**, 779 (2014).
- [103] C.-K. Chiu, J. C. Y. Teo, A. P. Schnyder, and S. Ryu, *Rev. Mod. Phys.* **88**, 035005 (2016).
- [104] C.-K. Chiu, H. Yao, and S. Ryu, *Phys. Rev. B* **88**, 075142 (2013).
- [105] C.-K. Chiu and A. P. Schnyder, *Phys. Rev. B* **90**, 205136 (2014).

- [106] See Supplementary Materials for more details which includes: (i) Hermitian and non-Hermitian symmetries; (ii) Symmetries and skin modes; (iii) Non-Hermitian Rice-Mele model; (iv) Chiral tunneling effect; (v) Mathematica code.
- [107] Z. Yang (in preparation).
- [108] When $r_n < 1$, it seems that the term r_n^{1-N} will tend to infinity in the limit of $N \rightarrow \infty$. However, in the Supplementary Materials, we show that the tunneling probability is bounded to less than 1, when the system is purely dissipative.

Supplemental Materials for “Non-Hermitian skin modes induced by on-site dissipations and chiral tunneling effect”

Yifei Yi^{1,2} and Zhesen Yang^{1,2*}

¹*Beijing National Laboratory for Condensed Matter Physics,
and Institute of Physics, Chinese Academy of Sciences, Beijing 100190, China and*

²*University of Chinese Academy of Sciences, Beijing 100049, China*

(Dated: March 5, 2020)

CONTENTS

I. Hermitian and non-Hermitian symmetries	2
A. Symmetry generators	2
1. Hermitian symmetries	2
2. Non-Hermitian symmetries	2
B. Symmetry ramifications	2
1. TRS	2
2. PHS	3
3. Other symmetries	3
C. Symmetry groups	4
1. Hermitian case	4
2. Non-Hermitian case	5
D. Symmetry constraint to the characteristic equation	5
1. TRS	5
2. TRS [†]	6
3. PHS	6
4. PHS [†]	7
5. IS	8
II. Symmetries and skin modes	8
A. Case. 1	8
B. Case. 2	9
1. $G_{\bar{\mathcal{T}}_{\pm}, (\mathcal{PT})_{\pm}}$	9
2. $G_{\bar{\mathcal{T}}_{\pm}, (\mathcal{PC})_{\pm}}$	10
3. $G_{\bar{\mathcal{T}}_{\pm}, (\mathcal{PC})_{\pm}}$	11
C. Case. 3	11
D. Case. 4	12
E. Numerical verification	13
III. Non-Hermitian Rice-Mele model	14
A. Phase diagram of spinless model	14
B. Spin $U(1)$ symmetry of the spinful model	17
IV. Chiral tunneling effect	18
A. Reviews of bi-orthogonal basis	18
1. The method to calculate the left eigenstates	19
B. Spinless model	19
1. Non-Bloch Hamiltonian and its solution	19
2. Open boundary Hamiltonian and its solution	20
3. Left eigenstate of the open boundary Hamiltonian	21

* yangzs@iphy.ac.cn

C. Local density of states	21
D. Tunneling probability	21
V. Mathematica code	23
References	23

I. HERMITIAN AND NON-HERMITIAN SYMMETRIES

A. Symmetry generators

1. Hermitian symmetries

In one-dimensional (1D) Hermitian system, there exist three nonspatial symmetries, time-reversal symmetry (TRS), particle-hole symmetry (PHS), and chiral symmetry (CS), and one spatial symmetry, inversion symmetry (IS). Here CS is a combination of TRS and PHS. Thus, the independent symmetry generators are TRS, PHS and IS. Based on these three independent generators, other symmetries can be obtained by combining two or three of them, that is

$$\mathcal{T}, \mathcal{C}, \mathcal{P} \quad \rightarrow \quad \mathcal{TC}, \mathcal{PT}, \mathcal{PC}, \mathcal{PTC}. \quad (1)$$

The constraints of these symmetries to the Bloch Hamiltonian are shown in Table. 1 in the main text. Note that in the Hermitian case, since the transpose operator \mathcal{K}^t and complex conjugate operator \mathcal{K}^* are equivalent due to $\mathcal{H} = \mathcal{H}^\dagger$, the PHS, which is defined by the transpose operator $\mathcal{C} = U_{\mathcal{C}}\mathcal{K}^t$, is equivalent to $\mathcal{C} = U_{\mathcal{C}}\mathcal{K}^*$ [1, 2]. Mathematically, the role of Hermitian symmetries can be classified by

$$(i) : k \rightarrow (k, -k), \quad (ii) : E \rightarrow (E, -E), \quad (iii) : \mathcal{H} \rightarrow (\mathcal{H} = \mathcal{H}^\dagger, \mathcal{H}^* = \mathcal{H}^t), \quad (2)$$

which implies there only exist $2 \times 2 \times 2 = 8$ group elements in all 1D Hermitian groups, including the 7 symmetries listed in Eq. 1 and the identity element I.

2. Non-Hermitian symmetries

For the non-Hermitian Hamiltonians, since $\mathcal{H} \neq \mathcal{H}^\dagger$, the role of non-Hermitian symmetries can be classified by

$$(i) : k \rightarrow (k, -k), \quad (ii) : E \rightarrow (E, -E), \quad (iii) : \mathcal{H} \rightarrow (\mathcal{H}, \mathcal{H}^*, \mathcal{H}^t, \mathcal{H}^\dagger). \quad (3)$$

This results $2 \times 2 \times 4 = 16$ different group elements in all the 1D non-Hermitian symmetry groups, which are listed in Table. 1 of the main text. Based on the three independent generators of the Hermitian case (TRS, PHS, and IS), there exist five independent generators in non-Hermitian case, namely, TRS, PHS, IS, anomalous time-reversal symmetry (TRS^\dagger), and anomalous particle-hole symmetry (PHS^\dagger). Using these five symmetries, other symmetries can be obtained by combining several of them, that is

$$\begin{aligned} I &= \mathcal{T}\bar{\mathcal{T}}\mathcal{C}\bar{\mathcal{C}}, \quad \mathcal{T} = \bar{\mathcal{T}}\mathcal{C}\bar{\mathcal{C}}, \quad \bar{\mathcal{T}} = \mathcal{T}\mathcal{C}\bar{\mathcal{C}}, \quad \mathcal{C} = \mathcal{T}\bar{\mathcal{T}}\bar{\mathcal{C}}, \quad \bar{\mathcal{C}} = \mathcal{T}\bar{\mathcal{T}}\mathcal{C}, \quad \mathcal{P} = \mathcal{P}\mathcal{T}\bar{\mathcal{T}}\bar{\mathcal{C}} \\ \mathcal{T}\bar{\mathcal{T}} &= \mathcal{C}\bar{\mathcal{C}}, \quad \mathcal{T}\mathcal{C} = \bar{\mathcal{T}}\bar{\mathcal{C}}, \quad \bar{\mathcal{T}}\mathcal{C} = \mathcal{T}\bar{\mathcal{C}}, \quad \mathcal{P}\mathcal{T} = \mathcal{P}\bar{\mathcal{T}}\mathcal{C}\bar{\mathcal{C}}, \quad \mathcal{P}\bar{\mathcal{T}} = \mathcal{P}\mathcal{T}\mathcal{C}\bar{\mathcal{C}}, \quad \mathcal{P}\mathcal{C} = \mathcal{P}\mathcal{T}\bar{\mathcal{T}}\bar{\mathcal{C}}, \quad \mathcal{P}\bar{\mathcal{C}} = \mathcal{P}\mathcal{T}\bar{\mathcal{T}}\mathcal{C}, \\ \mathcal{P}\mathcal{T}\bar{\mathcal{T}} &= \mathcal{P}\mathcal{C}\bar{\mathcal{C}}, \quad \mathcal{P}\mathcal{T}\mathcal{C} = \mathcal{P}\bar{\mathcal{T}}\bar{\mathcal{C}}, \quad \mathcal{P}\mathcal{T}\bar{\mathcal{C}} = \mathcal{P}\bar{\mathcal{T}}\mathcal{C}. \end{aligned} \quad (4)$$

Here “=” represents the corresponding symmetries are equivalent. The constraints of these symmetries to the Bloch Hamiltonian are shown in Table. 1 of the main text.

B. Symmetry ramifications

1. TRS

When the Hermitian system has TRS, which is represented by $\mathcal{T} = U_{\mathcal{T}}\mathcal{K}^*$, it must also preserve TRS^\dagger , which is represented by $\bar{\mathcal{T}} = U_{\mathcal{T}}\mathcal{K}^t$. The constraints to the Bloch Hamiltonian are

$$U_{\mathcal{T}}\mathcal{H}_s^*(k)U_{\mathcal{T}}^{-1} = U_{\mathcal{T}}\mathcal{H}_s^t(k)U_{\mathcal{T}}^{-1} = \mathcal{H}_s(-k). \quad (5)$$

Now, if we add the on-site dissipation to the Hermitian Hamiltonian,

$$\mathcal{H}_{s,eff}(k) = \mathcal{H}_s(k) + i\gamma\Gamma_0, \quad (6)$$

then, according to $\Gamma_0 = \Gamma_0^* = \Gamma_0^t$, the discussion can be classified by the commutation relation.

- $[U_{\mathcal{T}}, \Gamma_0] = 0$:

On the one hand, $U_{\mathcal{T}}\mathcal{H}_{s,eff}^*(k)U_{\mathcal{T}}^{-1} = U_{\mathcal{T}}[\mathcal{H}_s(k) + i\gamma\Gamma_0]^*U_{\mathcal{T}}^{-1} = U_{\mathcal{T}}[\mathcal{H}_s^*(k) - i\gamma\Gamma_0^*]U_{\mathcal{T}}^{-1} = \mathcal{H}_s(-k) - i\gamma\Gamma_0 \neq \mathcal{H}_{s,eff}(-k)$. This means TRS is broken by adding on-site dissipation.

On the other hand, $U_{\mathcal{T}}\mathcal{H}_{s,eff}^t(k)U_{\mathcal{T}}^{-1} = U_{\mathcal{T}}[\mathcal{H}_s(k) + i\gamma\Gamma_0]^tU_{\mathcal{T}}^{-1} = U_{\mathcal{T}}[\mathcal{H}_s^t(k) + i\gamma\Gamma_0^t]U_{\mathcal{T}}^{-1} = \mathcal{H}_s(-k) + i\gamma\Gamma_0 = \mathcal{H}_{s,eff}(-k)$. This means TRS[†] is preserved by adding on-site dissipation.

- $\{U_{\mathcal{T}}, \Gamma_0\} = 0$:

On the one hand, $U_{\mathcal{T}}\mathcal{H}_{s,eff}^*(k)U_{\mathcal{T}}^{-1} = U_{\mathcal{T}}[\mathcal{H}_s(k) + i\gamma\Gamma_0]^*U_{\mathcal{T}}^{-1} = U_{\mathcal{T}}[\mathcal{H}_s^*(k) - i\gamma\Gamma_0^*]U_{\mathcal{T}}^{-1} = \mathcal{H}_s(-k) + i\gamma\Gamma_0 = \mathcal{H}_{s,eff}(-k)$. This means TRS is preserved by adding on-site dissipation.

On the other hand, $U_{\mathcal{T}}\mathcal{H}_{s,eff}^t(k)U_{\mathcal{T}}^{-1} = U_{\mathcal{T}}[\mathcal{H}_s(k) + i\gamma\Gamma_0]^tU_{\mathcal{T}}^{-1} = U_{\mathcal{T}}[\mathcal{H}_s^t(k) + i\gamma\Gamma_0^t]U_{\mathcal{T}}^{-1} = \mathcal{H}_s(-k) - i\gamma\Gamma_0 \neq \mathcal{H}_{s,eff}(-k)$. This means TRS[†] is broken by adding on-site dissipation.

2. PHS

When the Hermitian system has PHS, which is represented by $\mathcal{C} = U_{\mathcal{C}}\mathcal{K}^t$, it must also preserve PHS[†], which is represented by $\bar{\mathcal{C}} = U_{\mathcal{C}}\mathcal{K}^*$. The constraints to the Bloch Hamiltonian are

$$U_{\mathcal{C}}\mathcal{H}_s^*(k)U_{\mathcal{C}}^{-1} = U_{\mathcal{C}}\mathcal{H}_s^t(k)U_{\mathcal{C}}^{-1} = -\mathcal{H}_s(-k). \quad (7)$$

Now, if we add the on-site dissipation to the Hermitian Hamiltonian,

$$\mathcal{H}_{s,eff}(k) = \mathcal{H}_s(k) + i\gamma\Gamma_0, \quad (8)$$

then, according to $\Gamma_0 = \Gamma_0^* = \Gamma_0^t$, the discussion can be classified by the commutation relation.

- $[U_{\mathcal{C}}, \Gamma_0] = 0$:

On the one hand, $U_{\mathcal{C}}\mathcal{H}_{s,eff}^t(k)U_{\mathcal{C}}^{-1} = U_{\mathcal{C}}[\mathcal{H}_s(k) + i\gamma\Gamma_0]^tU_{\mathcal{C}}^{-1} = U_{\mathcal{C}}[\mathcal{H}_s^t(k) + i\gamma\Gamma_0^t]U_{\mathcal{C}}^{-1} = -\mathcal{H}_s(-k) + i\gamma\Gamma_0 \neq -\mathcal{H}_{s,eff}(-k)$. This means PHS is broken by adding on-site dissipation.

On the other hand, $U_{\mathcal{C}}\mathcal{H}_{s,eff}^*(k)U_{\mathcal{C}}^{-1} = U_{\mathcal{C}}[\mathcal{H}_s(k) + i\gamma\Gamma_0]^*U_{\mathcal{C}}^{-1} = U_{\mathcal{C}}[\mathcal{H}_s^*(k) - i\gamma\Gamma_0^*]U_{\mathcal{C}}^{-1} = -\mathcal{H}_s(-k) - i\gamma\Gamma_0 = -\mathcal{H}_{s,eff}(-k)$. This means PHS[†] is preserved by adding on-site dissipation.

- $\{U_{\mathcal{C}}, \Gamma_0\} = 0$:

On the one hand, $U_{\mathcal{C}}\mathcal{H}_{s,eff}^t(k)U_{\mathcal{C}}^{-1} = U_{\mathcal{C}}[\mathcal{H}_s(k) + i\gamma\Gamma_0]^tU_{\mathcal{C}}^{-1} = U_{\mathcal{C}}[\mathcal{H}_s^t(k) + i\gamma\Gamma_0^t]U_{\mathcal{C}}^{-1} = -\mathcal{H}_s(-k) - i\gamma\Gamma_0 = -\mathcal{H}_{s,eff}(-k)$. This means PHS is preserved by adding on-site dissipation.

On the other hand, $U_{\mathcal{C}}\mathcal{H}_{s,eff}^*(k)U_{\mathcal{C}}^{-1} = U_{\mathcal{C}}[\mathcal{H}_s(k) + i\gamma\Gamma_0]^*U_{\mathcal{C}}^{-1} = U_{\mathcal{C}}[\mathcal{H}_s^*(k) - i\gamma\Gamma_0^*]U_{\mathcal{C}}^{-1} = -\mathcal{H}_s(-k) + i\gamma\Gamma_0 \neq -\mathcal{H}_{s,eff}(-k)$. This means PHS[†] is broken by adding on-site dissipation.

3. Other symmetries

For other symmetries, if they map $E \rightarrow E$, which include $I, \mathcal{P}, \mathcal{PT}, \mathcal{T}$, they are equivalent to the case of \mathcal{T} . To be more precise, when $[\Gamma_0, U_X] = 0$, the following symmetries without \mathcal{K}^* and \mathcal{K}^\dagger are preserved, namely, $I, \mathcal{PT}, \mathcal{P}, \bar{\mathcal{T}}$. When $\{\Gamma_0, U_X\} = 0$, the following symmetries with \mathcal{K}^* and \mathcal{K}^\dagger are preserved, namely, $\mathcal{T}, \mathcal{PT}, \mathcal{PT}\bar{\mathcal{T}}, \mathcal{T}$. On the other hand, if the symmetries map $E \rightarrow -E$, which include $\mathcal{TC}, \mathcal{PC}, \mathcal{PTC}, \mathcal{C}$, they are equivalent to the case of \mathcal{C} . To be more precise, when $[\Gamma_0, U_X] = 0$, the following symmetries with \mathcal{K}^* and \mathcal{K}^\dagger are preserved, namely, $\mathcal{TC}, \mathcal{PC}, \bar{\mathcal{C}}, \mathcal{C}, \mathcal{PTC}$. When $\{\Gamma_0, U_X\} = 0$, the following symmetries without \mathcal{K}^* and \mathcal{K}^\dagger are preserved, namely, $\bar{\mathcal{T}}\mathcal{C}, \mathcal{PC}, \mathcal{C}, \mathcal{PTC}$. This finally gives the results in Table. 1.

TABLE I. Hermitian symmetry classes. There exist three independent symmetry generators, TRS (\mathcal{T}), PHS (\mathcal{C}), and IS (\mathcal{P}). Here the red colors represent the Hermitian symmetry groups we concerned, which preserve TRS but break PHS.

Group generators	Symmetries	Group generators	Symmetries
I	$U_I = \mathcal{I}$	$\mathcal{P} = U_{\mathcal{P}}$	$U_{\mathcal{P}}^2 = 1$
$\mathcal{T} = U_{\mathcal{T}}\mathcal{K}^*$	$U_{\mathcal{T}}U_{\mathcal{T}}^* = \pm 1$	$\mathcal{P}\mathcal{T} = U_{\mathcal{P}}\mathcal{T}\mathcal{K}^*$	$U_{\mathcal{P}}\mathcal{T}U_{\mathcal{P}}^* = \pm 1$
$\mathcal{C} = U_{\mathcal{C}}\mathcal{K}^t$	$U_{\mathcal{C}}U_{\mathcal{C}}^* = \pm 1$	$\mathcal{P}\mathcal{C} = U_{\mathcal{P}}\mathcal{C}\mathcal{K}^t$	$U_{\mathcal{P}}\mathcal{C}U_{\mathcal{P}}^* = \pm 1$
$\mathcal{T}\mathcal{C} = U_{\mathcal{T}}\mathcal{C}\mathcal{K}^\dagger$	$U_{\mathcal{T}}^2 = 1$	$\mathcal{P}\mathcal{T}\mathcal{C} = U_{\mathcal{P}}\mathcal{T}\mathcal{C}\mathcal{K}^\dagger$	$(U_{\mathcal{P}}\mathcal{T}\mathcal{C})^2 = 1$
Group generators	Symmetries		
$\{\mathcal{P} = U_{\mathcal{P}}, \mathcal{T}\mathcal{C} = U_{\mathcal{T}}\mathcal{C}\mathcal{K}^\dagger\}$	$(U_{\mathcal{P}}U_{\mathcal{T}}\mathcal{C})^2 = \pm 1$		
$\{\mathcal{P} = U_{\mathcal{P}}, \mathcal{T} = U_{\mathcal{T}}\mathcal{K}^*\}$	$U_{\mathcal{T}}U_{\mathcal{T}}^* = \pm 1, (U_{\mathcal{P}}U_{\mathcal{T}})(U_{\mathcal{P}}U_{\mathcal{T}})^* = \pm 1$		
$\{\mathcal{P} = U_{\mathcal{P}}, \mathcal{C} = U_{\mathcal{C}}\mathcal{K}^t\}$	$U_{\mathcal{C}}U_{\mathcal{C}}^* = \pm 1, (U_{\mathcal{P}}U_{\mathcal{C}})(U_{\mathcal{P}}U_{\mathcal{C}})^* = \pm 1$		
$\{\mathcal{T} = U_{\mathcal{T}}\mathcal{K}^*, \mathcal{C} = U_{\mathcal{C}}\mathcal{K}^t\}$	$U_{\mathcal{T}}U_{\mathcal{T}}^* = \pm 1, U_{\mathcal{C}}U_{\mathcal{C}}^* = \pm 1$		
$\{\mathcal{T} = U_{\mathcal{T}}\mathcal{K}^*, \mathcal{P}\mathcal{C} = U_{\mathcal{P}}\mathcal{C}\mathcal{K}^t\}$	$U_{\mathcal{T}}U_{\mathcal{T}}^* = \pm 1, U_{\mathcal{P}}\mathcal{C}U_{\mathcal{P}}^* = \pm 1$		
$\{\mathcal{P}\mathcal{T} = U_{\mathcal{P}}\mathcal{T}\mathcal{K}^*, \mathcal{C} = U_{\mathcal{C}}\mathcal{K}^t\}$	$U_{\mathcal{P}}\mathcal{T}U_{\mathcal{P}}^* = \pm 1, U_{\mathcal{C}}U_{\mathcal{C}}^* = \pm 1$		
$\{\mathcal{P}\mathcal{T} = U_{\mathcal{P}}\mathcal{T}\mathcal{K}^*, \mathcal{P}\mathcal{C} = U_{\mathcal{P}}\mathcal{C}\mathcal{K}^t\}$	$U_{\mathcal{P}}\mathcal{T}U_{\mathcal{P}}^* = \pm 1, U_{\mathcal{P}}\mathcal{C}U_{\mathcal{P}}^* = \pm 1$		
Group generators	Symmetries		
$\{\mathcal{P} = U_{\mathcal{P}}, \mathcal{T} = U_{\mathcal{T}}\mathcal{K}^*, \mathcal{C} = U_{\mathcal{C}}\mathcal{K}^t\}$	$U_{\mathcal{T}}U_{\mathcal{T}}^* = \pm 1, U_{\mathcal{C}}U_{\mathcal{C}}^* = \pm 1, (U_{\mathcal{P}}U_{\mathcal{T}})(U_{\mathcal{P}}U_{\mathcal{T}})^* = \pm 1, (U_{\mathcal{P}}U_{\mathcal{C}})(U_{\mathcal{P}}U_{\mathcal{C}})^* = \pm 1$		

C. Symmetry groups

Before discussing the symmetry classifications, we first clarify the representations we used. If U_X (or $U_X\mathcal{K}$) is a representation of X , then, $e^{i\theta}U_X$ (or $e^{i\theta}U_X\mathcal{K}$) is also a representation of X . Furthermore, the additional phase does not restrict the forms of the Bloch Hamiltonian, since it can not change the commutation relation between some definite terms of the Hamiltonian. For example, for any given θ of $\mathcal{P} = e^{i\theta}\sigma_x$, the Hamiltonians with IS always have the following form $\mathcal{H}(k) = h_0(k)\sigma_0 + h_x(k)\sigma_x + h_y(k)\sigma_y + h_z(k)\sigma_z$, where $h_{0/x}(k) = h_{0/x}(-k)$ and $h_{y/z}(k) = -h_{y/z}(-k)$. Therefore, without loss of generality, the representations of non-Hermitian symmetries X can be chosen as

$$U_X, e^{i\theta}U_X\mathcal{K}^*, e^{i\theta}U_X\mathcal{K}^t, U_X\mathcal{K}^\dagger, \quad (9)$$

where U_X is a Hermitian unitary matrix. Therefore, the representations of X can be further classified as follows [2]

$$\begin{aligned} X = U_X \ \& \ U_X\mathcal{K}^\dagger \ \rightarrow U_X^2 = 1, \\ X = U_X\mathcal{K}^* \ \& \ U_X\mathcal{K}^t \ \rightarrow U_XU_X^* = \pm 1. \end{aligned} \quad (10)$$

1. Hermitian case

For the Hermitian case, all the symmetries can be generated by the following independent generators

$$\begin{aligned} \text{TRS } (\mathcal{T} = U_{\mathcal{T}}\mathcal{K}^*) : \quad & U_{\mathcal{T}}\mathcal{H}^*(k)U_{\mathcal{T}}^{-1} = \mathcal{H}(-k), \quad U_{\mathcal{T}}U_{\mathcal{T}}^* = \pm 1, \\ \text{PHS } (\mathcal{C} = U_{\mathcal{C}}\mathcal{K}^t) : \quad & U_{\mathcal{C}}\mathcal{H}^t(k)U_{\mathcal{C}}^{-1} = -\mathcal{H}(-k), \quad U_{\mathcal{C}}U_{\mathcal{C}}^* = \pm 1, \\ \text{IS } (\mathcal{P} = U_{\mathcal{P}}) : \quad & U_{\mathcal{P}}\mathcal{H}(k)U_{\mathcal{P}}^{-1} = \mathcal{H}(-k), \quad U_{\mathcal{P}}^2 = 1. \end{aligned} \quad (11)$$

The complete symmetry classification of 1D Hermitian Hamiltonian are shown in Table. I. There are two special notes we want to emphasize. One is $(U_{\mathcal{P}}U_{\mathcal{T}}\mathcal{C})^2 = \pm 1$, which is equivalent to $[\mathcal{P}, \mathcal{T}\mathcal{C}]_{\mp} = 1$. Proof: according to $\mathcal{P}\mathcal{T}\mathcal{C} \mp \mathcal{T}\mathcal{C}\mathcal{P} = U_{\mathcal{P}}U_{\mathcal{T}}\mathcal{C} \mp U_{\mathcal{T}}\mathcal{C}U_{\mathcal{P}} = 0$ and $U_{\mathcal{P}}^2 = U_{\mathcal{T}}^2 = 1$, one can obtain $U_{\mathcal{P}}U_{\mathcal{T}}\mathcal{C}U_{\mathcal{P}}U_{\mathcal{T}}\mathcal{C} = \pm 1$. The other is

$$U_{\mathcal{P}}XU_{\mathcal{P}}^* = -pU_XU_X^*, \quad (12)$$

where $X = \mathcal{T}, \mathcal{C}$ and $[\mathcal{P}, X]_p = 0$ with $p = \pm$. Here are the proof. Without loss of generality, we let $X = \mathcal{T}$.

- If $p = -1$, namely, $[\mathcal{P}, \mathcal{T}] = [\mathcal{P}, \mathcal{T}]_- = 0$, we have $\mathcal{P}\mathcal{T} - \mathcal{T}\mathcal{P} = 0 \rightarrow \mathcal{T} = \mathcal{P}\mathcal{T}\mathcal{P} \rightarrow e^{i\theta}U_{\mathcal{T}}\mathcal{K}^* = U_{\mathcal{P}}e^{i\theta}U_{\mathcal{T}}\mathcal{K}^*U_{\mathcal{P}} \rightarrow U_{\mathcal{T}} = U_{\mathcal{P}}U_{\mathcal{T}}U_{\mathcal{P}}^* \rightarrow U_{\mathcal{T}}U_{\mathcal{T}}^* = U_{\mathcal{P}}U_{\mathcal{T}}U_{\mathcal{P}}^*U_{\mathcal{T}}^* = (U_{\mathcal{P}}U_{\mathcal{T}})(U_{\mathcal{P}}U_{\mathcal{T}})^* = U_{\mathcal{P}\mathcal{T}}U_{\mathcal{P}\mathcal{T}}^*$.
- If $p = +1$, namely, $\{\mathcal{P}, \mathcal{T}\} = [\mathcal{P}, \mathcal{T}]_+ = 0$, we have $\mathcal{P}\mathcal{T} + \mathcal{T}\mathcal{P} = 0 \rightarrow \mathcal{T} = -\mathcal{P}\mathcal{T}\mathcal{P} \rightarrow e^{i\theta}U_{\mathcal{T}}\mathcal{K}^* = -U_{\mathcal{P}}e^{i\theta}U_{\mathcal{T}}\mathcal{K}^*U_{\mathcal{P}} \rightarrow U_{\mathcal{T}} = -U_{\mathcal{P}}U_{\mathcal{T}}U_{\mathcal{P}}^* \rightarrow U_{\mathcal{T}}U_{\mathcal{T}}^* = -U_{\mathcal{P}}U_{\mathcal{T}}U_{\mathcal{P}}^*U_{\mathcal{T}}^* = -(U_{\mathcal{P}}U_{\mathcal{T}})(U_{\mathcal{P}}U_{\mathcal{T}})^* = -U_{\mathcal{P}\mathcal{T}}U_{\mathcal{P}\mathcal{T}}^*$.

If $X = \mathcal{C}$, the proof are the same by using the fact $U_{\mathcal{C}}^* = U_{\mathcal{C}}^\dagger$.

According to Table. I, there exists 54 symmetry classes for the 1D Hermitian Hamiltonians. As discussed in the main text, we only focus on the systems preserving TRS but breaking PHS. According to Table. I, only the symmetry classes with red color will be discussed in the following section, namely, $G_{\mathcal{T}\pm}$, $G_{\mathcal{T}\pm, (\mathcal{P}\mathcal{T})\pm}$, $G_{\mathcal{T}\pm, (\mathcal{P}\mathcal{C})\pm}$.

2. Non-Hermitian case

For the non-Hermitian case, the symmetry ramification only depends on the commutation relation between the unitary part of the symmetry representation and the on-site dissipation term, namely,

$$\begin{aligned} Y = U_Y \quad &\rightarrow Y = U_Y \quad \text{or } \bar{Y} = U_Y\mathcal{K}^\dagger, \\ X = e^{i\theta}U_X\mathcal{K}^* \quad &\rightarrow X = e^{i\theta}U_X\mathcal{K}^* \quad \text{or } \bar{X} = e^{i\theta}U_X\mathcal{K}^t. \end{aligned} \quad (13)$$

Thus, the square relation can not be changed by adding the non-Hermitian term. For example, consider a Hermitian system with TRS, e.g. $\mathcal{T} = U_{\mathcal{T}}\mathcal{K}^*$ and $U_{\mathcal{T}}U_{\mathcal{T}}^* = -1$, then, if $[\Gamma_0, U_{\mathcal{T}}] = 0$, the non-Hermitian system must have TRS[†] with $\bar{\mathcal{T}} = U_{\mathcal{T}}\mathcal{K}^t$ and $U_{\mathcal{T}}U_{\mathcal{T}}^* = -1$; if $\{\Gamma_0, U_{\mathcal{T}}\} = 0$, the TRS is preserved in non-Hermitian systems with $\mathcal{T} = U_{\mathcal{T}}\mathcal{K}^*$ and $U_{\mathcal{T}}U_{\mathcal{T}}^* = -1$. Therefore, with the existence of on-site dissipation, besides $G_{\mathcal{T}\pm}$, $G_{\mathcal{T}\pm, (\mathcal{P}\mathcal{T})\pm}$, $G_{\mathcal{T}\pm, (\mathcal{P}\mathcal{C})\pm}$, the following 26 non-Hermitian symmetry groups can be ramified $G_{\bar{\mathcal{T}}\pm}$, $G_{\bar{\mathcal{T}}\pm, (\mathcal{P}\bar{\mathcal{T}})\pm}$, $G_{\bar{\mathcal{T}}\pm, (\mathcal{P}\mathcal{T})\pm}$, $G_{\bar{\mathcal{T}}\pm, (\mathcal{P}\bar{\mathcal{T}})\pm}$, $G_{\bar{\mathcal{T}}\pm, (\mathcal{P}\mathcal{C})\pm}$, $G_{\bar{\mathcal{T}}\pm, (\mathcal{P}\mathcal{C})\pm}$, $G_{\bar{\mathcal{T}}\pm, (\mathcal{P}\bar{\mathcal{C}})\pm}$.

D. Symmetry constraint to the characteristic equation

1. TRS

For the TRS, the constraint to the Bloch Hamiltonian with periodic boundary condition is

$$U_{\mathcal{T}}\mathcal{H}^*(-k)U_{\mathcal{T}}^{-1} = \mathcal{H}(k). \quad (14)$$

This implies the characteristic equation satisfying

$$\begin{aligned} f(k, E) &= \det[E - \mathcal{H}(k)] = \det[E - U_{\mathcal{T}}\mathcal{H}^*(-k)U_{\mathcal{T}}^{-1}] = \det[E - \mathcal{H}^*(-k)] \\ &= (\det[E^* - \mathcal{H}(-k)])^* = f^*(-k, E^*). \end{aligned} \quad (15)$$

Now suppose that the characteristic equation can be expressed as

$$f(k, E) = \sum_{l, m, n} c_{l, m, n} E^l (\sin k)^m (\cos k)^n. \quad (16)$$

Then, according to Eq. 15

$$\sum_{l, m, n} c_{l, m, n} E^l (\sin k)^m (\cos k)^n = \sum_{l, m, n} c_{l, m, n}^* E^l (-\sin k)^m (\cos k)^n, \quad (17)$$

one can obtain,

$$c_{l, m, n} = (-1)^m c_{l, m, n}^*. \quad (18)$$

This means

$$\lambda_{l, 2m_0, n} := c_{l, 2m_0, n} \text{ is real,} \quad i\lambda_{l, 2m_0+1, n} := c_{l, 2m_0+1, n} \text{ is imaginary,} \quad (19)$$

where m_0 is an integer. Now we extend $\beta = e^{ik}$ to the entire complex plane. The characteristic equation becomes

$$\begin{aligned} f(\beta, E) &= \sum_{l, m_0, n} \left[\lambda_{l, 2m_0, n} E^l \left(\frac{\beta^2 - 1}{2i\beta} \right)^{2m_0} \left(\frac{\beta^2 + 1}{2\beta} \right)^n + i\lambda_{l, 2m_0+1, n} E^l \left(\frac{\beta^2 - 1}{2i\beta} \right)^{2m_0+1} \left(\frac{\beta^2 + 1}{2\beta} \right)^n \right] \\ &= \sum_{l, m_0, n} \left[\lambda_{l, 2m_0, n} (E^*)^l \left(\frac{(\beta^*)^2 - 1}{2i\beta^*} \right)^{2m_0} \left(\frac{(\beta^*)^2 + 1}{2\beta^*} \right)^n + i\lambda_{l, 2m_0+1, n} (E^*)^l \left(\frac{(\beta^*)^2 - 1}{2i\beta^*} \right)^{2m_0+1} \left(\frac{(\beta^*)^2 + 1}{2\beta^*} \right)^n \right]^* \\ &= [f(\beta^*, E^*)]^*. \end{aligned} \quad (20)$$

Since $f(\beta, E) = [f(\beta^*, E^*)]^* = 0$, we finally obtain

$$f(\beta, E) = f(\beta^*, E^*). \quad (21)$$

2. TRS[†]

For the TRS[†], the constraint to the Bloch Hamiltonian with periodic boundary condition is

$$U_{\bar{\tau}} \mathcal{H}^t(-k) U_{\bar{\tau}}^{-1} = \mathcal{H}(k). \quad (22)$$

This implies the characteristic equation satisfying

$$f(k, E) = \det[E - \mathcal{H}(k)] = \det[E - U_{\bar{\tau}} \mathcal{H}^t(-k) U_{\bar{\tau}}^{-1}] = \det[E - \mathcal{H}^t(-k)] = \det[E - \mathcal{H}(-k)] = f(-k, E). \quad (23)$$

Now suppose that the characteristic equation can be expressed as

$$f(k, E) = \sum_{l, m, n} c_{l, m, n} E^l (\sin k)^m (\cos k)^n. \quad (24)$$

The constraint of Eq. 23 implies

$$c_{l, m, n} = (-1)^m c_{l, m, n}, \quad (25)$$

which is equivalent to

$$c_{l, 2m_0+1, n} = 0, \quad (26)$$

where m_0 is an integer. Now we extend $\beta = e^{ik}$ to the entire complex plane. The characteristic equation becomes

$$\begin{aligned} f(\beta, E) &= \sum_{l, m_0, n} c_{l, 2m_0, n} E^l \left(\frac{\beta^2 - 1}{2i\beta} \right)^{2m_0} \left(\frac{\beta^2 + 1}{2\beta} \right)^n \\ &= \sum_{l, m_0, n} c_{l, 2m_0, n} E^l \left(\frac{1 - \beta^2}{2i\beta} \right)^{2m_0} \left(\frac{\beta^2 + 1}{2\beta} \right)^n \\ &= f(1/\beta, E). \end{aligned} \quad (27)$$

3. PHS

For the PHS, the constraint to the Bloch Hamiltonian with periodic boundary condition is

$$-U_C \mathcal{H}^t(-k) U_C^{-1} = \mathcal{H}(k). \quad (28)$$

This implies the characteristic equation satisfying

$$f(k, E) = \det[E - \mathcal{H}(k)] = \det[E + U_C \mathcal{H}^t(-k) U_C^{-1}] = \det[E + \mathcal{H}(-k)] = (-1)^d \det[-E - \mathcal{H}(-k)] = (-1)^d f(-k, -E). \quad (29)$$

where d is the dimension of the matrix. Now suppose that the characteristic equation can be expressed as

$$f(k, E) = \sum_{l,m,n} c_{l,m,n} E^l (\sin k)^m (\cos k)^n. \quad (30)$$

The constraint of Eq. 29 implies

$$c_{l,m,n} = (-1)^{d+l+m} c_{l,m,n}, \quad (31)$$

Now we extend $\beta = e^{ik}$ to the entire complex plane. The characteristic equation becomes

$$\begin{aligned} f(\beta, E) &= \sum_{l,m,n} c_{l,m,n} E^l \left(\frac{\beta^2 - 1}{2i\beta} \right)^m \left(\frac{\beta^2 + 1}{2\beta} \right)^n \\ &= \sum_{l,m,n} (-1)^{d+l+m} c_{l,m,n} E^l \left(\frac{\beta^2 - 1}{2i\beta} \right)^m \left(\frac{\beta^2 + 1}{2\beta} \right)^n \\ &= (-1)^d \sum_{l,m,n} c_{l,m,n} (-E)^l \left(\frac{1 - \beta^2}{2i\beta} \right)^m \left(\frac{\beta^2 + 1}{2\beta} \right)^n \\ &= (-1)^d f(1/\beta, -E). \end{aligned} \quad (32)$$

However, in general, the matrix dimension of the Bloch Hamiltonian is even number, thus we finally obtain

$$f(\beta, E) = f(1/\beta, -E). \quad (33)$$

4. PHS[†]

For the PHS[†], the constraint to the Bloch Hamiltonian with periodic boundary condition is

$$-U_{\bar{c}} \mathcal{H}^*(-k) U_{\bar{c}}^{-1} = \mathcal{H}(k). \quad (34)$$

This implies the characteristic equation satisfying

$$\begin{aligned} f(k, E) &= \det[E - \mathcal{H}(k)] = \det[E + U_{\bar{c}} \mathcal{H}^*(-k) U_{\bar{c}}^{-1}] = \det[E + \mathcal{H}^*(-k)] \\ &= (-1)^d \det[-E - \mathcal{H}^*(-k)] = (-1)^d (\det[-E^* - \mathcal{H}(-k)])^* = (-1)^d f^*(-k, -E^*). \end{aligned} \quad (35)$$

where d is the dimension of the matrix. Now suppose that the characteristic equation can be expressed as

$$f(k, E) = \sum_{l,m,n} c_{l,m,n} E^l (\sin k)^m (\cos k)^n. \quad (36)$$

Then, according to Eq. 35

$$\sum_{l,m,n} c_{l,m,n} E^l (\sin k)^m (\cos k)^n = (-1)^d \sum_{l,m,n} c_{l,m,n}^* (-E)^l (-\sin k)^m (\cos k)^n, \quad (37)$$

one can obtain,

$$c_{l,m,n} = (-1)^{d+l+m} c_{l,m,n}^*. \quad (38)$$

Now we extend $\beta = e^{ik}$ to the entire complex plane. The characteristic equation becomes

$$\begin{aligned} f(\beta, E) &= \sum_{l,m,n} c_{l,m,n} E^l \left(\frac{\beta^2 - 1}{2i\beta} \right)^m \left(\frac{\beta^2 + 1}{2\beta} \right)^n \\ &= \sum_{l,m,n} (-1)^{d+l+m} c_{l,m,n}^* E^l \left(\frac{\beta^2 - 1}{2i\beta} \right)^m \left(\frac{\beta^2 + 1}{2\beta} \right)^n \\ &= (-1)^d \sum_{l,m,n} c_{l,m,n}^* (-E)^l \left(-\frac{\beta^2 - 1}{2i\beta} \right)^m \left(\frac{\beta^2 + 1}{2\beta} \right)^n \\ &= (-1)^d \sum_{l,m,n} \left[c_{l,m,n} (-E^*)^l \left(\frac{(\beta^*)^2 - 1}{2i\beta^*} \right)^m \left(\frac{(\beta^*)^2 + 1}{2\beta^*} \right)^n \right]^* \\ &= (-1)^d [f(\beta^*, -E^*)]^*. \end{aligned} \quad (39)$$

Since $f(\beta, E) = (-1)^d [f(\beta^*, -E^*)]^* = 0$, we finally obtain

$$f(\beta, E) = f(\beta^*, -E^*). \quad (40)$$

5. IS

For the IS, the constraint to the Bloch Hamiltonian with periodic boundary condition is

$$U_{\mathcal{P}} \mathcal{H}(-k) U_{\mathcal{P}}^{-1} = \mathcal{H}(k). \quad (41)$$

This implies the characteristic equation satisfying

$$f(k, E) = \det[E - \mathcal{H}(k)] = \det[E - U_{\mathcal{P}} \mathcal{H}(-k) U_{\mathcal{P}}^{-1}] = \det[E - \mathcal{H}(-k)] = f(-k, E). \quad (42)$$

Now suppose that the characteristic equation can be expressed as

$$f(k, E) = \sum_{l, m, n} c_{l, m, n} E^l (\sin k)^m (\cos k)^n. \quad (43)$$

The constraint of Eq. 42 implies

$$c_{l, m, n} = (-1)^m c_{l, m, n}, \quad (44)$$

which is equivalent to

$$c_{l, 2m_0+1, n} = 0, \quad (45)$$

where m is an integer. Now we extend $\beta = e^{ik}$ to the entire complex plane. The characteristic equation becomes

$$\begin{aligned} f(\beta, E) &= \sum_{l, m_0, n} c_{l, 2m_0, n} E^l \left(\frac{\beta^2 - 1}{2i\beta} \right)^{2m_0} \left(\frac{\beta^2 + 1}{2\beta} \right)^n \\ &= \sum_{l, m_0, n} c_{l, 2m_0, n} E^l \left(\frac{1 - \beta^2}{2i\beta} \right)^{2m_0} \left(\frac{\beta^2 + 1}{2\beta} \right)^n \\ &= f(1/\beta, E). \end{aligned} \quad (46)$$

II. SYMMETRIES AND SKIN MODES

In this section, we will derive and give the numerical verification of the emergence or the absence of skin modes in the non-Hermitian symmetry groups we concerned, namely, $G_{\mathcal{T}_{\pm}}$, $G_{\bar{\mathcal{T}}_{\pm}}$, $G_{\mathcal{T}_{\pm}, (\mathcal{PT})_{\pm}}$, $G_{\mathcal{T}_{\pm}, (\mathcal{PT})_{\pm}}$, $G_{\bar{\mathcal{T}}_{\pm}, (\mathcal{PT})_{\pm}}$, $G_{\bar{\mathcal{T}}_{\pm}, (\mathcal{PT})_{\pm}}$, $G_{\mathcal{T}_{\pm}, (\mathcal{PC})_{\pm}}$, $G_{\mathcal{T}_{\pm}, (\mathcal{PC})_{\pm}}$, $G_{\bar{\mathcal{T}}_{\pm}, (\mathcal{PC})_{\pm}}$, $G_{\bar{\mathcal{T}}_{\pm}, (\mathcal{PC})_{\pm}}$. The procedure of derivation can be summarized as follows: (i) we first write down the GBZ condition based on Table. 2 in the main text; (ii) we then find all the symmetry related non-Bloch waves; (iii) we finally check whether the GBZ condition and the symmetry related non-Bloch waves imply $|\beta_p| = |\beta_{p+1}| = 1$ (or $|\beta_{p-1}| = |\beta_p| = |\beta_{p+1}| = |\beta_{p+2}| = 1$). According to Table. 1 in the main text, only $\bar{\mathcal{T}}_+$ and \mathcal{P} implies $f(\beta, E) = f(1/\beta, E)$. Therefore, the discussion is classified as follows.

A. Case. 1

The first case is that G does not contain $\bar{\mathcal{T}}_+$ nor \mathcal{P} , which includes

$$G_{\mathcal{T}_{\pm}}, G_{\mathcal{T}_{\pm}, (\mathcal{PT})_{\pm}}, G_{\mathcal{T}_{\pm}, (\mathcal{PC})_{\pm}}, G_{\mathcal{T}_{\pm}, (\mathcal{PC})_{\pm}}. \quad (47)$$

The absence of $\bar{\mathcal{T}}_+$ and \mathcal{P} implies the existence of skin modes.

B. Case. 2

The second case is that G only contains $\bar{\mathcal{T}}$, which includes

$$G_{\bar{\mathcal{T}}_{\pm}}, G_{\bar{\mathcal{T}}_{\pm}, (\mathcal{PT})_{\pm}}, G_{\bar{\mathcal{T}}_{\pm}, (\mathcal{PC})_{\pm}}, G_{\bar{\mathcal{T}}_{\pm}, (\mathcal{PC})_{\pm}}. \quad (48)$$

Here $G_{\bar{\mathcal{T}}_{\pm}}$ has been discussed in the main text. We only focus on the latter three cases.

1. $G_{\bar{\mathcal{T}}_{\pm}, (\mathcal{PT})_{\pm}}$

- $G_{\bar{\mathcal{T}}_{+}, (\mathcal{PT})_{+}}$:

According to the GBZ condition $|\beta_p| = |\beta_{p+1}|$ and the transformation of non-Bloch waves

$$\begin{array}{ccc} |\beta, E\rangle & \xrightarrow{\bar{\mathcal{T}}_{+}} & |1/\beta, E\rangle \\ (\mathcal{PT})_{+} \downarrow & & \downarrow (\mathcal{PT})_{+} \\ |1/\beta^*, E^*\rangle & \xrightarrow{\bar{\mathcal{T}}_{+}} & |\beta^*, E^*\rangle \end{array}$$

one can obtain the conclusion “GBZ=BZ”. To be more precise, the superposition of $|k, E\rangle$ and $|-k, E\rangle$ forms the eigenstate of the open boundary Hamiltonian with eigenenergy E .

- $G_{\bar{\mathcal{T}}_{+}, (\mathcal{PT})_{-}}$:

According to the GBZ condition (i) for $E \in \mathbb{R}$, $|\beta_{p-1}| = |\beta_p|$ & $|\beta_{p+1}| = |\beta_{p+2}|$; (ii) for $E \in \mathbb{C}$, $|\beta_p| = |\beta_{p+1}|$ and the transformation of non-Bloch waves

$$\begin{array}{ccc} |\beta, E, \uparrow\rangle & \xrightarrow{\bar{\mathcal{T}}_{+}} & |1/\beta, E, \uparrow\rangle \\ (\mathcal{PT})_{-} \downarrow & & \downarrow (\mathcal{PT})_{-} \\ |1/\beta^*, E^*, \downarrow\rangle & \xrightarrow{\bar{\mathcal{T}}_{+}} & |\beta^*, E^*, \downarrow\rangle \end{array}$$

one can obtain the conclusion “GBZ=BZ”. To be more precise, for the nonreal eigenvalue, the eigenstate is a superposition of the following two Bloch waves, $|k, E, \uparrow\rangle$ and $|-k, E, \uparrow\rangle$; for the real eigenvalue, the open boundary eigenstate has a two fold degeneracy, which means the eigenstate is a superposition of the following four Bloch waves, $|k, E, \uparrow\rangle$, $|-k, E, \uparrow\rangle$, $|k', E, \downarrow\rangle$, $|-k', E, \downarrow\rangle$. We note that with the existence of $(\mathcal{PT})_{-}$ symmetry, the characteristic equation satisfies $f(\beta, E) = f(1/\beta^*, E^*)$, in which the order of β must be a even number. This means for any given E and $f(\beta, E) = 0$, there must exist even number of solutions. On the other hand, for any $E \in \mathbb{R}$, if $\beta = re^{i\theta}$ is a solution, $\beta = e^{i\theta}/r$ is also a solution, which implies the solutions must come in pairs. Specially, when $r = 1$, the solutions are also formed pairs, namely, $\beta = e^{ik}$ and $\beta = e^{ik'}$. This explains why there exist $|k', E, \downarrow\rangle$, $|-k', E, \downarrow\rangle$ in the above discussion.

- $G_{\bar{\mathcal{T}}_{-}, (\mathcal{PT})_{+}}$:

According to the GBZ condition $|\beta_{p-1}| = |\beta_p|$ & $|\beta_{p+1}| = |\beta_{p+2}|$ and the transformation of non-Bloch waves

$$\begin{array}{ccc} |\beta, E, \uparrow\rangle & \xrightarrow{\bar{\mathcal{T}}_{-}} & |1/\beta, E, \downarrow\rangle \\ (\mathcal{PT})_{+} \downarrow & & \downarrow (\mathcal{PT})_{+} \\ |1/\beta^*, E^*, \uparrow\rangle & \xrightarrow{\bar{\mathcal{T}}_{-}} & |\beta^*, E^*, \downarrow\rangle \end{array}$$

one can obtain the conclusion (i) for the real spectra, “GBZ=BZ”; (ii) for the nonreal spectral, “GBZ≠BZ”. This means the eigenstates of the nonreal spectra are skin modes. To be more precise, for the real eigenvalue, the open boundary eigenstate is two fold degeneracy due to $\bar{\mathcal{T}}_{-}$, and a superposition of the following four Bloch waves, $|k, E, \uparrow\rangle$, $|-k, E, \downarrow\rangle$, $|k', E, \uparrow\rangle$, $|-k', E, \downarrow\rangle$. We further note that, due to the existence of \mathcal{PT} symmetry, the system can belong to the \mathcal{PT} -unbroken phase, whose spectra are all reals. In this \mathcal{PT} -unbroken phase, it is impossible to have skin modes. However, when \mathcal{PT} symmetry is spontaneously broken in the system, skin modes emerge simultaneously.

- $G_{\bar{\mathcal{T}}_-, (\mathcal{PT})_-}$:

According to the GBZ condition $|\beta_{p-1}| = |\beta_p|$ & $|\beta_{p+1}| = |\beta_{p+2}|$ and the transformation of non-Bloch waves

$$\begin{array}{ccc} |\beta, E, \uparrow\rangle & \xrightarrow{\bar{\mathcal{T}}_-} & |1/\beta, E, \downarrow\rangle \\ (\mathcal{PT})_- \downarrow & & \downarrow (\mathcal{PT})_- \\ |1/\beta^*, E^*, \downarrow\rangle & \xrightarrow{\bar{\mathcal{T}}_-} & |\beta^*, E^*, \uparrow\rangle \end{array}$$

one can obtain the conclusion (i) for the real spectra, “GBZ=BZ”; (ii) for the nonreal spectral, “GBZ \neq BZ”. This case is similar to the above case $G_{\bar{\mathcal{T}}_-, (\mathcal{PT})_+}$.

2. $G_{\bar{\mathcal{T}}_{\pm}, (\mathcal{PC})_{\pm}}$

- $G_{\bar{\mathcal{T}}_+, (\mathcal{PC})_+}$:

According to the GBZ condition $|\beta_p| = |\beta_{p+1}|$ and the transformation of non-Bloch waves

$$\begin{array}{ccc} |\beta, E\rangle & \xrightarrow{\bar{\mathcal{T}}_+} & |1/\beta, E\rangle \\ (\mathcal{PC})_+ \downarrow & & \downarrow (\mathcal{PC})_+ \\ |\beta, -E\rangle & \xrightarrow{\bar{\mathcal{T}}_+} & |1/\beta, -E\rangle \end{array}$$

one can obtain the conclusion “GBZ=BZ”. To be more precise, for any eigenvalue in the complex plane, the corresponding eigenstate is a superposition of $|k, E\rangle$ and $|-k, E\rangle$.

- $G_{\bar{\mathcal{T}}_+, (\mathcal{PC})_-}$:

According to the GBZ condition $|\beta_p| = |\beta_{p+1}|$ and the transformation of non-Bloch waves

$$\begin{array}{ccc} |\beta, E, \uparrow\rangle & \xrightarrow{\bar{\mathcal{T}}_+} & |1/\beta, E, \uparrow\rangle \\ (\mathcal{PC})_- \downarrow & & \downarrow (\mathcal{PC})_- \\ |\beta, -E, \downarrow\rangle & \xrightarrow{\bar{\mathcal{T}}_+} & |1/\beta, -E, \downarrow\rangle \end{array}$$

one can obtain the conclusion “GBZ=BZ”. To be more precise, for any eigenvalue in the complex plane, the corresponding eigenstate is a superposition of $|k, E, \uparrow\rangle$ and $|-k, E, \uparrow\rangle$.

- $G_{\bar{\mathcal{T}}_-, (\mathcal{PC})_+}$:

According to the GBZ condition $|\beta_{p-1}| = |\beta_p|$ & $|\beta_{p+1}| = |\beta_{p+2}|$ and the transformation of non-Bloch waves

$$\begin{array}{ccc} |\beta, E, \uparrow\rangle & \xrightarrow{\bar{\mathcal{T}}_-} & |1/\beta, E, \downarrow\rangle \\ (\mathcal{PC})_+ \downarrow & & \downarrow (\mathcal{PC})_+ \\ |\beta, -E, \uparrow\rangle & \xrightarrow{\bar{\mathcal{T}}_-} & |1/\beta, -E, \downarrow\rangle \end{array}$$

one can obtain the conclusion “GBZ \neq BZ”. This means the system can have skin modes.

- $G_{\bar{\mathcal{T}}_-, (\mathcal{PC})_-}$:

According to the GBZ condition $|\beta_{p-1}| = |\beta_p|$ & $|\beta_{p+1}| = |\beta_{p+2}|$ and the transformation of non-Bloch waves

$$\begin{array}{ccc} |\beta, E, \uparrow\rangle & \xrightarrow{\bar{\mathcal{T}}_-} & |1/\beta, E, \downarrow\rangle \\ (\mathcal{PC})_- \downarrow & & \downarrow (\mathcal{PC})_- \\ |\beta, -E, \downarrow\rangle & \xrightarrow{\bar{\mathcal{T}}_-} & |1/\beta, -E, \uparrow\rangle \end{array}$$

one can obtain the conclusion “GBZ \neq BZ”. This means the system can have skin modes.

3. $G_{\bar{\mathcal{T}}_{\pm},(\mathcal{P}\bar{\mathcal{C}})_{\pm}}$ • $G_{\bar{\mathcal{T}}_+, (\mathcal{P}\bar{\mathcal{C}})_+}$:

According to the GBZ condition $|\beta_p| = |\beta_{p+1}|$ and the transformation of non-Bloch waves

$$\begin{array}{ccc} |\beta, E\rangle & \xrightarrow{\bar{\mathcal{T}}_+} & |1/\beta, E\rangle \\ (\mathcal{P}\bar{\mathcal{C}})_+ \downarrow & & \downarrow (\mathcal{P}\bar{\mathcal{C}})_+ \\ |1/\beta^*, -E^*\rangle & \xrightarrow{\bar{\mathcal{T}}_+} & |\beta^*, -E^*\rangle \end{array}$$

one can obtain the conclusion “GBZ=BZ”. To be more precise, for any eigenvalue in the complex plane, the corresponding eigenstate is a superposition of $|k, E\rangle$ and $|-k, E\rangle$.

• $G_{\bar{\mathcal{T}}_+, (\mathcal{P}\bar{\mathcal{C}})_-}$:

According to the GBZ condition (i) for $iE \in \mathbb{R}$, $|\beta_{p-1}| = |\beta_p|$ & $|\beta_{p+1}| = |\beta_{p+2}|$; (ii) for $E \in \mathbb{C}$, $|\beta_p| = |\beta_{p+1}|$ and the transformation of non-Bloch waves

$$\begin{array}{ccc} |\beta, E, \uparrow\rangle & \xrightarrow{\bar{\mathcal{T}}_+} & |1/\beta, E, \uparrow\rangle \\ (\mathcal{P}\bar{\mathcal{C}})_- \downarrow & & \downarrow (\mathcal{P}\bar{\mathcal{C}})_- \\ |1/\beta^*, -E^*, \downarrow\rangle & \xrightarrow{\bar{\mathcal{T}}_+} & |\beta^*, -E^*, \downarrow\rangle \end{array}$$

one can obtain the conclusion “GBZ=BZ”. To be more precise, for the nonimaginary eigenvalue, the eigenstate is a superposition of $|k, E, \uparrow\rangle, |-k, E, \uparrow\rangle$; for the imaginary eigenvalue, the eigenstate is a superposition of $|k, E, \uparrow\rangle, |-k, E, \uparrow\rangle, |k', E, \downarrow\rangle, |-k', E, \downarrow\rangle$.

• $G_{\bar{\mathcal{T}}_-, (\mathcal{P}\bar{\mathcal{C}})_+}$:

According to the GBZ condition $|\beta_{p-1}| = |\beta_p|$ & $|\beta_{p+1}| = |\beta_{p+2}|$ and the transformation of non-Bloch waves

$$\begin{array}{ccc} |\beta, E, \uparrow\rangle & \xrightarrow{\bar{\mathcal{T}}_-} & |1/\beta, E, \downarrow\rangle \\ (\mathcal{P}\bar{\mathcal{C}})_+ \downarrow & & \downarrow (\mathcal{P}\bar{\mathcal{C}})_+ \\ |1/\beta^*, -E^*, \uparrow\rangle & \xrightarrow{\bar{\mathcal{T}}_-} & |\beta^*, -E^*, \downarrow\rangle \end{array}$$

one can obtain the conclusion (i) for the imaginary spectra, “GBZ=BZ”; (ii) for the nonimaginary spectral, “GBZ \neq BZ”. To be more precise, for the imaginary eigenvalue, the eigenstate is a superposition of the following four Bloch waves, $|k, E, \uparrow\rangle, |-k, E, \uparrow\rangle, |k', E, \downarrow\rangle, |-k', E, \downarrow\rangle$.

• $G_{\bar{\mathcal{T}}_-, (\mathcal{P}\bar{\mathcal{C}})_-}$:

According to the GBZ condition $|\beta_{p-1}| = |\beta_p|$ & $|\beta_{p+1}| = |\beta_{p+2}|$ and the transformation of non-Bloch waves

$$\begin{array}{ccc} |\beta, E, \uparrow\rangle & \xrightarrow{\bar{\mathcal{T}}_-} & |1/\beta, E, \downarrow\rangle \\ (\mathcal{P}\bar{\mathcal{C}})_- \downarrow & & \downarrow (\mathcal{P}\bar{\mathcal{C}})_- \\ |1/\beta^*, -E^*, \downarrow\rangle & \xrightarrow{\bar{\mathcal{T}}_-} & |\beta^*, -E^*, \uparrow\rangle \end{array}$$

one can obtain the conclusion (i) for the imaginary spectra, “GBZ=BZ”; (ii) for the nonimaginary spectral, “GBZ \neq BZ”. This case is similar to the above case $G_{\bar{\mathcal{T}}_-, (\mathcal{P}\bar{\mathcal{C}})_+}$.

C. Case 3

The third case is that G only contains \mathcal{P} , which includes

$$G_{\mathcal{T}_{\pm}, (\mathcal{P}\mathcal{T})_{\pm}}. \quad (49)$$

- $G_{\mathcal{T}_+, (\mathcal{PT})_+}$:

According to the GBZ condition $|\beta_p| = |\beta_{p+1}|$ and the transformation of non-Bloch waves

$$\begin{array}{ccc} |\beta, E\rangle & \xrightarrow{\mathcal{T}_+} & |\beta^*, E^*\rangle \\ (\mathcal{PT})_+ \downarrow & & \downarrow (\mathcal{PT})_+ \\ |1/\beta^*, E^*\rangle & \xrightarrow{\mathcal{T}_+} & |1/\beta, E\rangle \end{array}$$

one can obtain the conclusion “GBZ=BZ”. To be more precise, for any eigenvalue in the complex plane, the corresponding eigenstate is a superposition of $|k, E\rangle$ and $|-k, E\rangle$.

- $G_{\mathcal{T}_+, (\mathcal{PT})_-}$:

According to the GBZ condition (i) for $E \in \mathbb{R}$, $|\beta_{p-1}| = |\beta_p|$ & $|\beta_{p+1}| = |\beta_{p+2}|$; (ii) for $E \in \mathbb{C}$, $|\beta_p| = |\beta_{p+1}|$ and the transformation of non-Bloch waves

$$\begin{array}{ccc} |\beta, E, \uparrow\rangle & \xrightarrow{\mathcal{T}_+} & |\beta^*, E^*, \uparrow\rangle \\ (\mathcal{PT})_- \downarrow & & \downarrow (\mathcal{PT})_- \\ |1/\beta^*, E^*, \downarrow\rangle & \xrightarrow{\mathcal{T}_+} & |1/\beta, E, \downarrow\rangle \end{array}$$

one can obtain the conclusion “GBZ=BZ”. To be more precise, for the nonreal eigenvalue, the eigenstate is a superposition of the following two Bloch waves, $|k, E, \uparrow\rangle$ and $|-k, E, \downarrow\rangle$; for the real eigenvalue, the open boundary eigenstate is a superposition of the following four Bloch waves, $|k, E, \uparrow\rangle$, $|-k, E, \downarrow\rangle$, $|k', E, \uparrow\rangle$, $|-k', E, \downarrow\rangle$. We also note that for any nonreal E in the complex plane, the solution is a superposition of two spin bands. The phenomena that the open boundary eigenstate is a superposition of two distinct bands has been reported in Ref. [3].

- $G_{\mathcal{T}_-, (\mathcal{PT})_+}$:

According to the GBZ condition (i) for $E \in \mathbb{R}$, $|\beta_{p-1}| = |\beta_p| = |\beta_{p+1}| = |\beta_{p+2}|$; (ii) for $E \in \mathbb{C}$, $|\beta_p| = |\beta_{p+1}|$ and the transformation of non-Bloch waves

$$\begin{array}{ccc} |\beta, E, \uparrow\rangle & \xrightarrow{\mathcal{T}_-} & |\beta^*, E^*, \downarrow\rangle \\ (\mathcal{PT})_+ \downarrow & & \downarrow (\mathcal{PT})_+ \\ |1/\beta^*, E^*, \uparrow\rangle & \xrightarrow{\mathcal{T}_-} & |1/\beta, E, \downarrow\rangle \end{array}$$

one can obtain the conclusion “GBZ=BZ”. This case is similar to the above case $G_{\mathcal{T}_+, (\mathcal{PT})_-}$.

- $G_{\mathcal{T}_-, (\mathcal{PT})_-}$:

According to the GBZ condition (i) for $E \in \mathbb{R}$, $|\beta_{p-1}| = |\beta_p| = |\beta_{p+1}| = |\beta_{p+2}|$; (ii) for $E \in \mathbb{C}$, $|\beta_p| = |\beta_{p+1}|$ and the transformation of non-Bloch waves

$$\begin{array}{ccc} |\beta, E, \uparrow\rangle & \xrightarrow{\mathcal{T}_-} & |\beta^*, E^*, \downarrow\rangle \\ (\mathcal{PT})_- \downarrow & & \downarrow (\mathcal{PT})_- \\ |1/\beta^*, E^*, \downarrow\rangle & \xrightarrow{\mathcal{T}_-} & |1/\beta, E, \uparrow\rangle \end{array}$$

one can obtain the conclusion “GBZ=BZ”. To be more precise, for the nonreal eigenvalue, the eigenstate is a superposition of the following two Bloch waves, $|k, E, \uparrow\rangle$ and $|-k, E, \uparrow\rangle$; for the real eigenvalue, the open boundary eigenstate is a superposition of the following four Bloch waves, $|k, E, \uparrow\rangle$, $|-k, E, \uparrow\rangle$, $|k', E, \downarrow\rangle$, $|-k', E, \downarrow\rangle$.

D. Case. 4

The last case is that G contains both $\bar{\mathcal{T}}_+$ and \mathcal{P} , which includes

$$G_{\bar{\mathcal{T}}_{\pm}, (\mathcal{PT})_{\pm}}. \quad (50)$$

- $G_{\bar{\mathcal{T}}_+, (\mathcal{P}\bar{\mathcal{T}})_+}$:

According to the GBZ condition $|\beta_p| = |\beta_{p+1}|$ and the transformation of non-Bloch waves

$$\begin{array}{ccc} |\beta, E\rangle & \xrightarrow{\bar{\mathcal{T}}_+} & |1/\beta, E\rangle \\ (\mathcal{P}\bar{\mathcal{T}})_+ \downarrow & & \downarrow (\mathcal{P}\bar{\mathcal{T}})_+ \\ |\beta, E\rangle & \xrightarrow{\bar{\mathcal{T}}_+} & |1/\beta, E\rangle \end{array}$$

one can obtain the conclusion “GBZ=BZ”. To be more precise, for any eigenvalue in the complex plane, the corresponding eigenstate is a superposition of $|k, E\rangle$ and $|-k, E\rangle$.

- $G_{\bar{\mathcal{T}}_+, (\mathcal{P}\bar{\mathcal{T}})_-}$:

According to the GBZ condition $|\beta_{p-1}| = |\beta_p| = |\beta_{p+1}| = |\beta_{p+2}|$ and the transformation of non-Bloch waves

$$\begin{array}{ccc} |\beta, E, \uparrow\rangle & \xrightarrow{\bar{\mathcal{T}}_+} & |1/\beta, E, \uparrow\rangle \\ (\mathcal{P}\bar{\mathcal{T}})_- \downarrow & & \downarrow (\mathcal{P}\bar{\mathcal{T}})_- \\ |\beta, E, \downarrow\rangle & \xrightarrow{\bar{\mathcal{T}}_+} & |1/\beta, E, \downarrow\rangle \end{array}$$

one can obtain the conclusion “GBZ=BZ”. To be more precise, for any eigenvalue in the complex plane, the corresponding eigenstate is a superposition of $|k, E, \uparrow\rangle$, $|-k, E, \uparrow\rangle$, $|k, E, \downarrow\rangle$, $|-k, E, \downarrow\rangle$.

- $G_{\bar{\mathcal{T}}_-, (\mathcal{P}\bar{\mathcal{T}})_+}$:

According to the GBZ condition $|\beta_{p-1}| = |\beta_p|$ & $|\beta_{p+1}| = |\beta_{p+2}|$ and the transformation of non-Bloch waves

$$\begin{array}{ccc} |\beta, E, \uparrow\rangle & \xrightarrow{\bar{\mathcal{T}}_-} & |1/\beta, E, \downarrow\rangle \\ (\mathcal{P}\bar{\mathcal{T}})_+ \downarrow & & \downarrow (\mathcal{P}\bar{\mathcal{T}})_+ \\ |\beta, E, \uparrow\rangle & \xrightarrow{\bar{\mathcal{T}}_-} & |1/\beta, E, \downarrow\rangle \end{array}$$

one can obtain the conclusion “GBZ \neq BZ”.

- $G_{\bar{\mathcal{T}}_-, (\mathcal{P}\bar{\mathcal{T}})_-}$:

According to the GBZ condition $|\beta_{p-1}| = |\beta_p| = |\beta_{p+1}| = |\beta_{p+2}|$ and the transformation of non-Bloch waves

$$\begin{array}{ccc} |\beta, E, \uparrow\rangle & \xrightarrow{\bar{\mathcal{T}}_-} & |1/\beta, E, \downarrow\rangle \\ (\mathcal{P}\bar{\mathcal{T}})_- \downarrow & & \downarrow (\mathcal{P}\bar{\mathcal{T}})_- \\ |\beta, E, \downarrow\rangle & \xrightarrow{\bar{\mathcal{T}}_-} & |1/\beta, E, \uparrow\rangle \end{array}$$

one can obtain the conclusion “GBZ=BZ”. To be more precise, for any eigenvalue in the complex plane, the corresponding eigenstate is a superposition of $|k, E, \uparrow\rangle$, $|-k, E, \uparrow\rangle$, $|k, E, \downarrow\rangle$, $|-k, E, \downarrow\rangle$.

In summary, skin modes are absent when G contains $\bar{\mathcal{T}}_+$, or \mathcal{P} with an exceptional case, namely, $G_{\bar{\mathcal{T}}_-, (\mathcal{P}\bar{\mathcal{T}})_+}$, where the skin modes emerge with the presence of IS.

E. Numerical verification

In order to verify the above conclusion, we provide a complete numerical calculation for all symmetry groups we concerned. We consider a four-band Bloch Hamiltonian

$$\mathcal{H}(k) = \sum_{\mu\nu} h_{\mu\nu}(k) \sigma_\mu \otimes \tau_\nu. \quad (51)$$

The representations of the symmetries are shown in Table II and III. Under the restriction of these symmetries, $h_{\mu\nu}(k)$ can be even or odd functions. In the numerical calculation, the even/odd functions are chosen to be

$$h_{\mu\nu}^{\text{even}}(k) = a_{\mu\nu} + b_{\mu\nu} \cos k + c_{\mu\nu} \cos^2 k \quad (52)$$

and

$$h_{\mu\nu}^{\text{odd}}(k) = e_{\mu\nu} \sin k + f_{\mu\nu} \sin^3 k. \quad (53)$$

For the real parameters, they are chosen to be random numbers in the region $[-10, 10]$; for the complex parameters, both the real and the imaginary parts are chosen to be random in the region $[-10, 10]$. The existence of skin modes can be indicated by the discrepancy between periodic/open boundary spectra shown in the next page (gray/black points).

TABLE II. Non-Hermitian symmetry classes we concerned

Group generators	\mathcal{T}	$\bar{\mathcal{T}}$
$U_X^{-1}\mathcal{H}(k)U_X =$	$\mathcal{H}^*(-k)$	$\mathcal{H}^t(-k)$
Representations	$\mathcal{T} = \mathcal{K}^*$	$\bar{\mathcal{T}} = \mathcal{K}^t$
	$\mathcal{T} = s_y \mathcal{K}^*$	$\bar{\mathcal{T}} = s_y \mathcal{K}^t$

TABLE III. Non-Hermitian symmetry classes we concerned.

Group generators	$(\mathcal{T}, \mathcal{PT})$	$(\bar{\mathcal{T}}, \mathcal{P}\bar{\mathcal{T}})$	$(\mathcal{T}, \mathcal{P}\bar{\mathcal{T}})$	$(\bar{\mathcal{T}}, \mathcal{PT})$
$U_X^{-1}\mathcal{H}(k)U_X =$	$(\mathcal{H}^*(-k), \mathcal{H}^*(k))$	$(\mathcal{H}^t(-k), \mathcal{H}^t(k))$	$(\mathcal{H}^*(-k), \mathcal{H}^t(k))$	$(\mathcal{H}^t(-k), \mathcal{H}^*(k))$
Representations	$\mathcal{T} = \mathcal{K}^*, \mathcal{PT} = \sigma_x \mathcal{K}^*$	$\bar{\mathcal{T}} = \mathcal{K}^t, \mathcal{P}\bar{\mathcal{T}} = \sigma_x \mathcal{K}^t$	$\mathcal{T} = \mathcal{K}^*, \mathcal{P}\bar{\mathcal{T}} = \sigma_x \mathcal{K}^t$	$\bar{\mathcal{T}} = \mathcal{K}^t, \mathcal{PT} = \sigma_x \mathcal{K}^*$
	$\mathcal{T} = \mathcal{K}^*, \mathcal{PT} = \sigma_y \mathcal{K}^*$	$\bar{\mathcal{T}} = \mathcal{K}^t, \mathcal{P}\bar{\mathcal{T}} = \sigma_y \mathcal{K}^t$	$\mathcal{T} = \mathcal{K}^*, \mathcal{P}\bar{\mathcal{T}} = \sigma_y \mathcal{K}^t$	$\bar{\mathcal{T}} = \mathcal{K}^t, \mathcal{PT} = \sigma_y \mathcal{K}^*$
	$\mathcal{T} = s_y \mathcal{K}^*, \mathcal{PT} = \sigma_x s_y \mathcal{K}^*$	$\bar{\mathcal{T}} = s_y \mathcal{K}^t, \mathcal{P}\bar{\mathcal{T}} = \sigma_x s_y \mathcal{K}^t$	$\mathcal{T} = s_y \mathcal{K}^*, \mathcal{P}\bar{\mathcal{T}} = \sigma_x s_y \mathcal{K}^t$	$\bar{\mathcal{T}} = s_y \mathcal{K}^t, \mathcal{PT} = \sigma_x s_y \mathcal{K}^*$
	$\mathcal{T} = s_y \mathcal{K}^*, \mathcal{PT} = \sigma_y s_y \mathcal{K}^*$	$\bar{\mathcal{T}} = s_y \mathcal{K}^t, \mathcal{P}\bar{\mathcal{T}} = \sigma_y s_y \mathcal{K}^t$	$\mathcal{T} = s_y \mathcal{K}^*, \mathcal{P}\bar{\mathcal{T}} = \sigma_y s_y \mathcal{K}^t$	$\bar{\mathcal{T}} = s_y \mathcal{K}^t, \mathcal{PT} = \sigma_y s_y \mathcal{K}^*$
Group generators	$\mathcal{T}, \mathcal{PC}$	$(\mathcal{T}, \mathcal{P}\bar{\mathcal{C}})$	$(\bar{\mathcal{T}}, \mathcal{PC})$	$(\bar{\mathcal{T}}, \mathcal{P}\bar{\mathcal{C}})$
$U_X^{-1}\mathcal{H}(k)U_X =$	$(\mathcal{H}^*(-k), -\mathcal{H}^t(k))$	$(\mathcal{H}^*(-k), -\mathcal{H}^*(k))$	$(\mathcal{H}^t(-k), -\mathcal{H}^t(k))$	$(\mathcal{H}^t(-k), -\mathcal{H}^*(k))$
Representations	$\mathcal{T} = \mathcal{K}^*, \mathcal{PC} = \sigma_x \mathcal{K}^t$	$\mathcal{T} = \mathcal{K}^*, \mathcal{P}\bar{\mathcal{C}} = \sigma_x \mathcal{K}^*$	$\bar{\mathcal{T}} = \mathcal{K}^t, \mathcal{PC} = \sigma_x \mathcal{K}^t$	$\bar{\mathcal{T}} = \mathcal{K}^t, \mathcal{P}\bar{\mathcal{C}} = \sigma_x \mathcal{K}^*$
	$\mathcal{T} = \mathcal{K}^*, \mathcal{PC} = \sigma_y \mathcal{K}^t$	$\mathcal{T} = \mathcal{K}^*, \mathcal{P}\bar{\mathcal{C}} = \sigma_y \mathcal{K}^*$	$\bar{\mathcal{T}} = \mathcal{K}^t, \mathcal{PC} = \sigma_y \mathcal{K}^t$	$\bar{\mathcal{T}} = \mathcal{K}^t, \mathcal{P}\bar{\mathcal{C}} = \sigma_y \mathcal{K}^*$
	$\mathcal{T} = s_y \mathcal{K}^*, \mathcal{PC} = \sigma_x s_y \mathcal{K}^t$	$\mathcal{T} = s_y \mathcal{K}^*, \mathcal{P}\bar{\mathcal{C}} = \sigma_x s_y \mathcal{K}^*$	$\bar{\mathcal{T}} = s_y \mathcal{K}^t, \mathcal{PC} = \sigma_x s_y \mathcal{K}^t$	$\bar{\mathcal{T}} = s_y \mathcal{K}^t, \mathcal{P}\bar{\mathcal{C}} = \sigma_x s_y \mathcal{K}^*$
	$\mathcal{T} = s_y \mathcal{K}^*, \mathcal{PC} = \sigma_y s_y \mathcal{K}^t$	$\mathcal{T} = s_y \mathcal{K}^*, \mathcal{P}\bar{\mathcal{C}} = \sigma_y s_y \mathcal{K}^*$	$\bar{\mathcal{T}} = s_y \mathcal{K}^t, \mathcal{PC} = \sigma_y s_y \mathcal{K}^t$	$\bar{\mathcal{T}} = s_y \mathcal{K}^t, \mathcal{P}\bar{\mathcal{C}} = \sigma_y s_y \mathcal{K}^*$

III. NON-HERMITIAN RICE-MELE MODEL

In order to make the Supplemental Materials self-contained, the Rice-Mele model is shown as follow

$$\mathcal{H}_{\text{RM}}(k) = (t_1 + t_2 \cos k) \sigma_x + t_2 \sin k \sigma_y + \mu \sigma_z. \quad (54)$$

When $\mu = 0$, the model reduces to the SSH model.

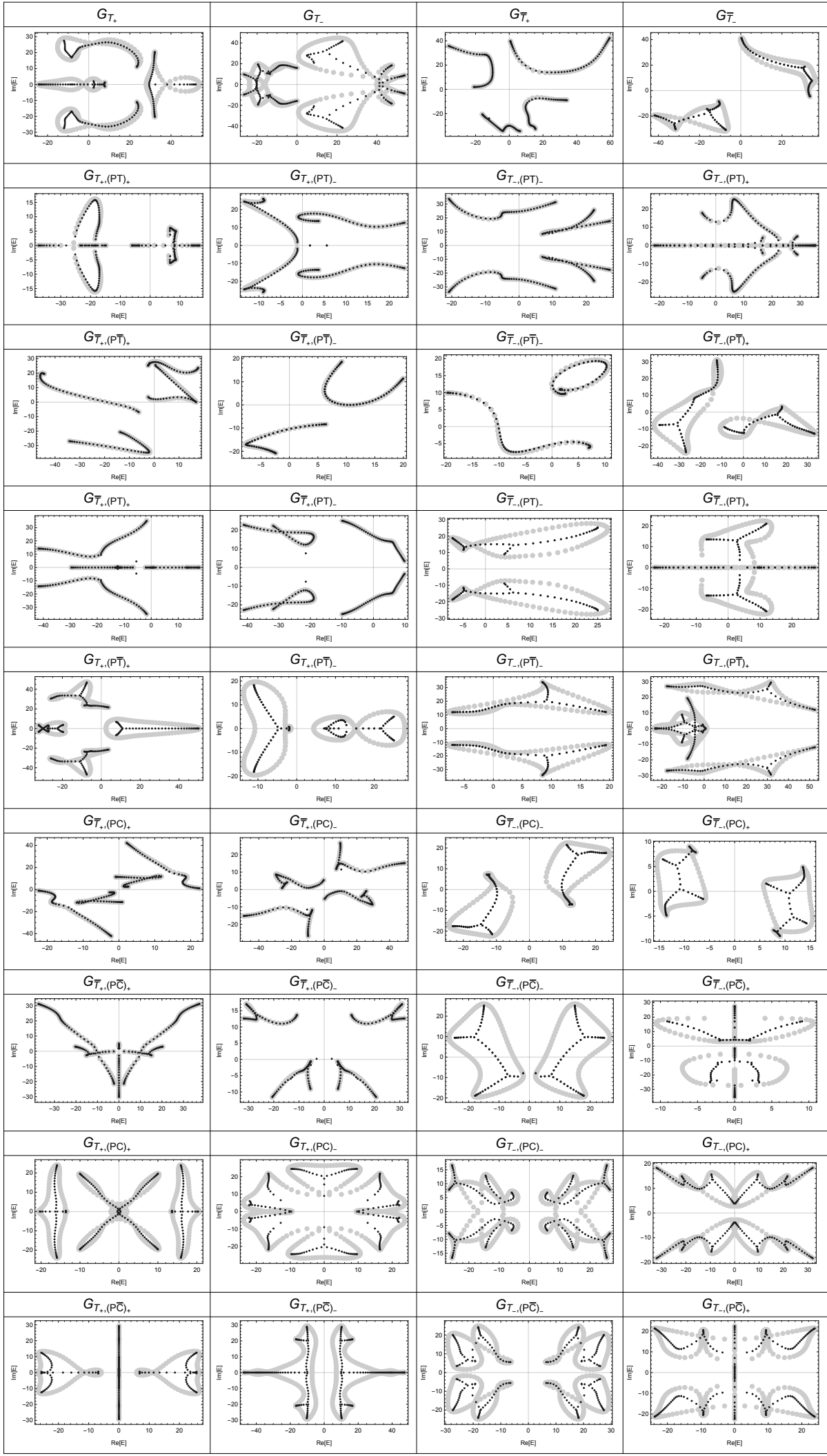
A. Phase diagram of spinless model

In the main text, we mentioned that regardless the value of μ , the skin modes always exist when $\lambda t_1 t_2 \neq 0$. Now we show this. The Bloch Hamiltonian of the spinless model we proposed in the main text has the following form

$$\mathcal{H}_{\text{spinless}}(k) = \mathcal{H}_{\text{RM}}(k) + \lambda \sin k \sigma_z + i\gamma \sigma_z, \quad (55)$$

where λ is the strength of π -flux, which breaks the TRS when $\gamma = 0$. The existence of skin modes can be predicted by the winding number [4, 5]

$$\nu(E_0) = \frac{1}{2\pi i} \int_0^{2\pi} dk \partial_k \ln \det[\mathcal{H}_{\text{spinless}}(k) - E_0]. \quad (56)$$



It should be noted that the above winding number formula depends on the choice of E_0 . The statement of the existence of skin modes is claimed as follow:

If there exist a $E_0 \in \mathbb{C}$ such that the winding number is nonzero, then, there must exist skin modes.

An equivalent statement is that [4]

If the area of the parametric curve defined as follow

$$k \rightarrow (\text{Re}[\det[\mathcal{H}_{\text{spinless}}(k)]], \text{Im}[\det[\mathcal{H}_{\text{spinless}}(k)]]) \quad (57)$$

is nonzero, then, there must exist skin modes.

The reason is that if the area is nonzero, one can always find a point E_0 in the region contributing to the area, such that the winding number is nonzero. Since the second statement is easy to apply, we will use it to calculate the phase diagram. The determinant of $\mathcal{H}_{\text{spinless}}(k)$ can be expressed as

$$\det[\mathcal{H}_{\text{spinless}}(k)] = \frac{\lambda^2}{2} \cos 2k - 2\lambda\mu \sin k - 2t_1 t_2 \cos k + (\gamma^2 - t_1^2 - t_2^2 - \mu^2 - \frac{\lambda^2}{2}) - i(2\lambda\gamma \sin k + 2\gamma\mu). \quad (58)$$

In order to have a zero area, any point of $(\text{Re}[\det[\mathcal{H}_{\text{spinless}}(k)]], \text{Im}[\det[\mathcal{H}_{\text{spinless}}(k)]])$ in the complex plane must be covered twice with opposite moving directions as k evolves, as shown in Fig. 1.

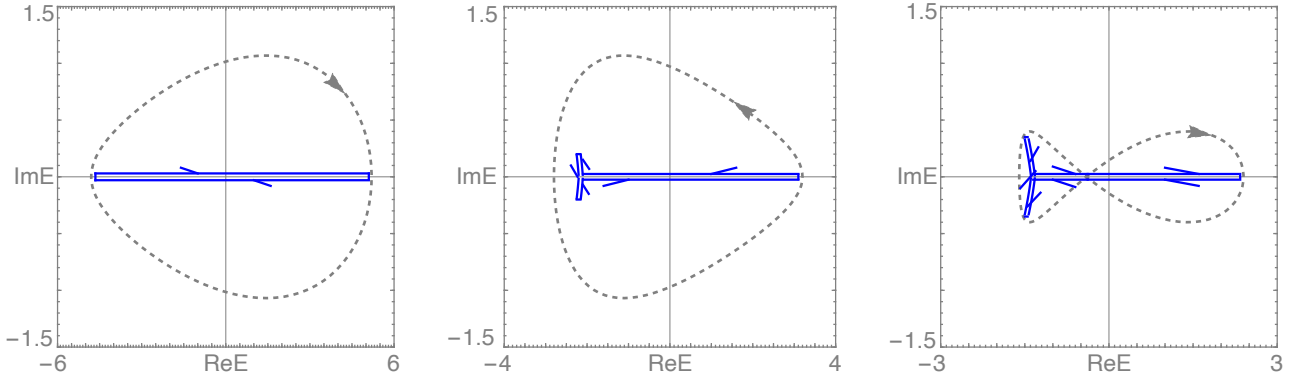


FIG. 1. Several examples of the zero and nonzero area curves. The blue ones represent the nonzero area cures. The arrows shows the moving direction as k evolves. One can notice that any point on the cure must be covered twice with opposite moving directions.

- If the imaginary part is k independent, the area must be zero. In this case, we require

$$\lambda\gamma = 0. \quad (59)$$

Since γ is the only non-Hermitian term we added, it can not be zero. Therefore, in order to satisfy the condition, λ must be zero. This means the preservation of TRS.

- If $\lambda\gamma \neq 0$, the following values of k correspond to the same imaginary part, namely, k and $\pm(2n+1)\pi - k$. Putting these values into the real part, according to $\cos 2k = \cos 2(\pm(2n+1)\pi - k)$, $\cos k \neq \cos(\pm(2n+1)\pi - k)$, one can notice that when

$$t_1 t_2 \neq 0, \quad (60)$$

k and $\pm(2n+1)\pi - k$ do not correspond to the same real parts. This means the area of the curve can not be zero, since the mapping from $k \in [-\pi, \pi]$ to $\det[\mathcal{H}_{\text{spinless}}(k)]$ is a one-to-one mapping.

- If $\lambda\gamma \neq 0$ but $t_1 t_2 = 0$, the area must be zero, since $\partial_k \det[\mathcal{H}_{\text{spinless}}(k)]|_{k_0} \neq \partial_k \det[\mathcal{H}_{\text{spinless}}(k)]|_{\pm(2n+1)\pi - k_0}$. This means the moving direction of the two points k_0 and $\pm(2n+1)\pi - k_0$ are not the same. The contribution to the winding number is canceled.

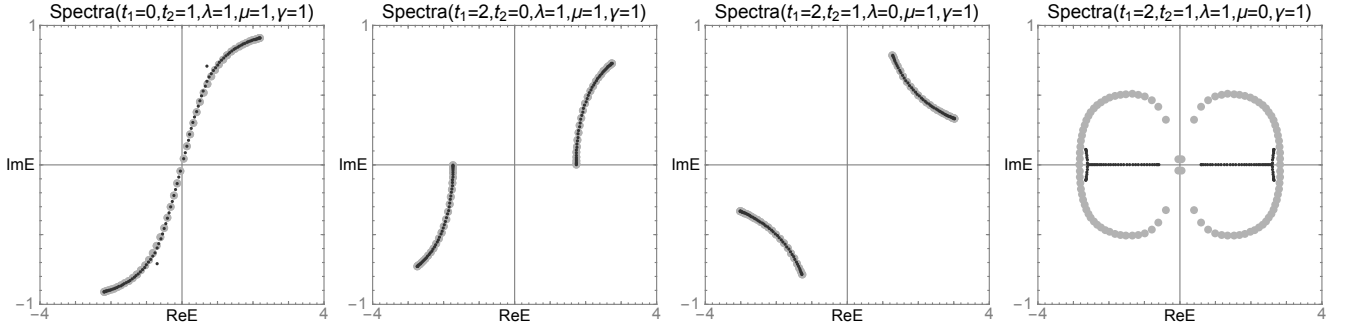


FIG. 2. Comparison between the open/periodic boundary spectra of the spinless model Eq. 55 with different parameters. The gray/black points represent the periodic/open boundary spectra.

In summary, the skin modes always exist with when $\lambda t_1 t_2 \neq 0$. As shown in Fig. 2, the numerical calculation also supports our analysis. Especially, when $\mu = 0$, as the right one of Fig. 2, on the one hand, the Rice-Mele model reduces to SSH model; on the other hand, the system also has skin modes. Indeed, the above analysis shows that the emergence of skin modes does not depend on the value of μ . This means the time-reversal-breaking SSH model can also have skin modes.

B. Spin $U(1)$ symmetry of the spinful model

The Bloch Hamiltonian of the spinful model is

$$\begin{aligned}\mathcal{H}_{\text{spinful}}(k) &= \mathcal{H}_{\text{RM}}(k)s_0 + \mathcal{H}_{\text{soc}}(k) + i\gamma\sigma_z s_0, \\ \mathcal{H}_{\text{soc}}(k) &= \lambda_I \sin k\sigma_z s_z - \lambda_R \sigma_y (s_x - \sqrt{3}s_y)/2.\end{aligned}\quad (61)$$

When $\lambda_R = 0$, the above model also has spin $U(1)$ symmetry. This mean the Bloch Hamiltonian can be reduced to two spin blocks,

$$\mathcal{H}_{\uparrow/\downarrow}(k) = \mathcal{H}_{\text{RM}}(k) \pm \lambda_I \sin k\sigma_z + i\gamma\sigma_z. \quad (62)$$

Under the following parameters, $t_1 = \lambda_I = 2, t_2 = \mu = \gamma = 1$, the spin up block Hamiltonian reduces to the spinless model discussed in the main text, namely, Fig. 1 in the main text. For the spin down block, we show the corresponding spectra, GBZ and auxiliary GBZ in Fig. 3. One can notice the GBZ is larger than 1. The Mathematica code for the calculation of auxiliary GBZ with nonzero λ_R is shown in the last section of the Supplemental Materials.

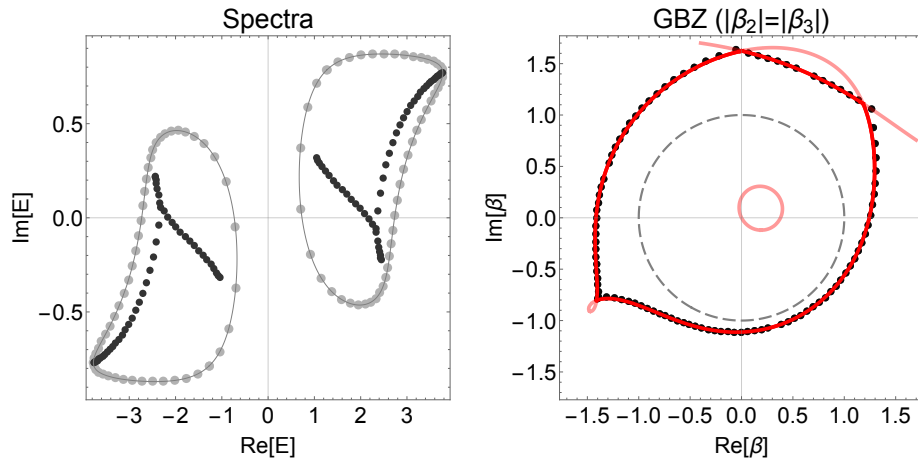


FIG. 3. (a) shows the open (black points) and periodic (gray points) boundary spectra of $\mathcal{H}_\downarrow(k)$ with the following parameters $t_1 = \lambda_I = 2, t_2 = \mu = \gamma = 1$. (b) shows the corresponding GBZ (black points) and auxiliary GBZ (red lines).

IV. CHIRAL TUNNELING EFFECT

A. Reviews of bi-orthogonal basis

Consider the following non-Hermitian Hamiltonian

$$\mathcal{H}_{eff} = \mathcal{H} + i\Gamma \quad \mathcal{H}_{eff}^\dagger = \mathcal{H} - i\Gamma \quad (63)$$

with the following eigenequations

$$\begin{aligned} \mathcal{H}_{eff}|\psi_n^R\rangle &= E_n|\psi_n^R\rangle, & \langle\psi_n^R|\mathcal{H}_{eff}^\dagger &= E_n^*\langle\psi_n^R|, \\ \mathcal{H}_{eff}^\dagger|\psi_n^L\rangle &= E_n^*\langle\psi_n^L|, & \langle\psi_n^L|\mathcal{H}_{eff} &= E_n\langle\psi_n^L| \end{aligned} \quad (64)$$

We assume there is no degeneracy in the following discussion. Consider two right eigenstates $|\psi_n^R\rangle$ and $|\psi_m^R\rangle$, according to $2\mathcal{H} = \mathcal{H}_{eff} + \mathcal{H}_{eff}^\dagger$ and $2i\Gamma = \mathcal{H}_{eff} - \mathcal{H}_{eff}^\dagger$, we have

$$\langle\psi_m^R|2\mathcal{H}|\psi_n^R\rangle = \langle\psi_m^R|(\mathcal{H}_{eff} + \mathcal{H}_{eff}^\dagger)|\psi_n^R\rangle = (E_n + E_m^*)\langle\psi_m^R|\psi_n^R\rangle \quad (65)$$

which in general results

$$\langle\psi_m^R|\psi_n^R\rangle = 2\frac{\langle\psi_m^R|\mathcal{H}|\psi_n^R\rangle}{E_m^* + E_n} = 2i\frac{\langle\psi_m^R|\Gamma|\psi_n^R\rangle}{E_n - E_m^*} \neq 0 \quad (66)$$

This means in general, the right eigenstates do not satisfy the orthogonal relation. On the other hand,

$$\langle\psi_m^L|\mathcal{H}_{eff}|\psi_n^R\rangle = E_n\langle\psi_m^L|\psi_n^R\rangle = E_m\langle\psi_m^L|\psi_n^R\rangle \quad (67)$$

Thus if $E_m \neq E_n$, $\langle\psi_m^L|\psi_n^R\rangle$ must be zero. As a result, we obtain the following identity operator

$$\sum_n \frac{|\psi_n^R\rangle\langle\psi_n^L|}{\langle\psi_n^L|\psi_n^R\rangle} = \mathbb{1}, \quad \sum_n \frac{|\psi_n^L\rangle\langle\psi_n^R|}{\langle\psi_n^R|\psi_n^L\rangle} = \mathbb{1}. \quad (68)$$

Notice that the above equations are true regardless of the choice of left/right normalization condition, namely, they are invariant under the following transformation

$$|\psi_n^R\rangle \rightarrow A_n|\psi_n^R\rangle, \quad |\psi_n^L\rangle \rightarrow B_n|\psi_n^L\rangle, \quad A_n, B_n \in \mathbb{C}. \quad (69)$$

Therefore, without loss of generality, we can choose the following bi-orthogonal normalization condition in the following discussion

$$\langle\psi_m^L|\psi_n^R\rangle = \delta_{mn}. \quad (70)$$

Under this condition, the Hamiltonian can be expressed as

$$\mathcal{H}_{eff} = \sum_n E_n|\psi_n^R\rangle\langle\psi_n^L|, \quad \mathcal{H}_{eff}^\dagger = \sum_n E_n^*|\psi_n^L\rangle\langle\psi_n^R|; \quad (71)$$

the time-evolution operator can be expressed as

$$U_{eff}(t) = e^{-i\mathcal{H}_{eff}t} = \sum_n e^{-iE_n t}|\psi_n^R\rangle\langle\psi_n^L|, \quad U_{eff}^\dagger(t) = e^{i\mathcal{H}_{eff}^\dagger t} = \sum_n e^{iE_n^* t}|\psi_n^L\rangle\langle\psi_n^R|; \quad (72)$$

and the corresponding Green's function can be expressed as

$$G(\omega) = \frac{1}{\omega - \mathcal{H}_{eff}} = \sum_n \frac{|\psi_n^R\rangle\langle\psi_n^L|}{\omega - E_n}. \quad (73)$$

1. *The method to calculate the left eigenstates*

Mathematically, the left eigenstates are called the dual base of the right eigenstates. We now show how to calculate them if we know all the right eigenstates. We first write down the eigenequations in the matrix form,

$$\mathcal{H}_{eff}\psi_n^R = E_n\psi_n^R, \quad \mathcal{H}_{eff}^\dagger\psi_n^L = E_n^*\psi_n^L, \quad (74)$$

where $\psi_n^{R/L}$ are column vectors, which can be expressed as

$$\psi_n^R = (\psi_{1,n}^R, \psi_{2,n}^R, \dots, \psi_{N-1,n}^R, \psi_{N,n}^R)^t, \quad \psi_n^L = (\psi_{1,n}^L, \psi_{2,n}^L, \dots, \psi_{N-1,n}^L, \psi_{N,n}^L)^t, \quad (75)$$

where $n = 1, 2, \dots, N$. Now define matrix

$$A = (\psi_1^L, \psi_2^L, \dots, \psi_{N-1}^L, \psi_N^L), \quad B = (\psi_1^R, \psi_2^R, \dots, \psi_{N-1}^R, \psi_N^R). \quad (76)$$

According to the bi-orthogonal normalization condition, we have

$$A^\dagger B = \mathbb{1} \quad \rightarrow \quad A = (B^{-1})^\dagger. \quad (77)$$

The column of matrix A are the corresponding left eigenstates.

B. Spinless model

1. *Non-Bloch Hamiltonian and its solution*

We now focus on the spinless model discussed in the main text, whose non-Bloch Hamiltonian can be obtained from the Bloch Hamiltonian $\mathcal{H}_{\text{spinless}}(k)$ by replacing e^{ik} with β , namely $\mathcal{H}_{\text{spinless}}(\beta = e^{ik})$, which has the following form

$$\mathcal{H}_{\text{spinless}}(\beta) = \begin{pmatrix} \mu + i\gamma - i\lambda(\beta - 1/\beta)/2 & t_1 + t_2/\beta \\ t_1 + t_2\beta & -\mu - i\gamma + i\lambda(\beta - 1/\beta)/2 \end{pmatrix}. \quad (78)$$

Define $h_z(\beta) = \mu + i\gamma - i\lambda(\beta - 1/\beta)/2$, according to the eigenequations

$$\mathcal{H}_{\text{spinless}}(\beta)u_\pm^R(\beta) = E_\pm(\beta)u_\pm^R(\beta), \quad \mathcal{H}_{\text{spinless}}^\dagger(\beta)u_\pm^L(\beta) = [E_\pm(\beta)]^*u_\pm^L(\beta), \quad (79)$$

one can obtain the eigenvalues

$$E_\pm(\beta) = \pm E(\beta) = \pm\sqrt{t_1^2 + t_2^2 + t_1 t_2(\beta + 1/\beta) + h_z^2(\beta)}, \quad (80)$$

and the corresponding right eigenstates

$$\begin{aligned} u_+^R(\beta) &= [h_z(\beta) + E(\beta), (t_1 + t_2\beta)]^t, \\ u_-^R(\beta) &= [h_z(\beta) - E(\beta), (t_1 + t_2\beta)]^t, \end{aligned} \quad (81)$$

Based on the above method, the corresponding left eigenstates are

$$\begin{aligned} u_+^L(\beta) &= \frac{1}{2E^*(\beta)(t_1 + t_2\beta^*)} [t_1 + t_2\beta^*, E^*(\beta) - h_z^*(\beta)]^t \\ u_-^L(\beta) &= \frac{1}{2E^*(\beta)(t_1 + t_2\beta^*)} [-(t_1 + t_2\beta^*), E^*(\beta) + h_z^*(\beta)]^t \end{aligned} \quad (82)$$

where $h_z^*(\beta) = \mu - i\gamma + i\lambda(\beta^* - 1/\beta^*)/2$. One can check that the above eigenstates are indeed the left eigenstates. Depending on the normalization condition of right eigenstates, when $\gamma = 0$, $u_\pm^L(\beta)$ can be equal to $u_\pm^R(\beta)$ up to a normalization factor. We note that if $\gamma \neq 0$, this kind of one-to-one correspondence between $u_\pm^L(\beta)$ and $u_\pm^R(\beta)$ would fail, and a left eigenstate would depend on the whole set of right eigenstates.

2. Open boundary Hamiltonian and its solution

We now focus on the open boundary condition, the real space Hamiltonian of the spinless models is

$$H_{\text{spinless}} = \begin{pmatrix} i\gamma + \mu & t_1 & -i\lambda & 0 & \dots & 0 & 0 & 0 & 0 \\ t_1 & -i\gamma - \mu & t_2 & i\lambda & \dots & 0 & 0 & 0 & 0 \\ i\lambda & t_2 & i\gamma + \mu & t_1 & \dots & 0 & 0 & 0 & 0 \\ 0 & -i\lambda & t_1 & -i\gamma - \mu & \dots & 0 & 0 & 0 & 0 \\ \dots & \dots \\ 0 & 0 & 0 & 0 & \dots & i\gamma + \mu & t_1 & -i\lambda & 0 \\ 0 & 0 & 0 & 0 & \dots & t_1 & -i\gamma - \mu & t_2 & i\lambda \\ 0 & 0 & 0 & 0 & \dots & i\lambda & t_2 & i\gamma + \mu & t_1 \\ 0 & 0 & 0 & 0 & \dots & 0 & -i\lambda & t_1 & -i\gamma - \mu \end{pmatrix} \quad (83)$$

In order to solve the open boundary spinless Hamiltonian with large N , we first need to solve the bulk equation, which is the non-Bloch Hamiltonian solved in the above subsection. Since in general, the eigenstate of H_{spinless} is a superposition of non-Bloch waves, we use $\psi_{n,\beta}^R$ to label the eigenstate. In contrast, $\psi_{n,k}^R$ is used to label a superposition of several conventional Bloch waves

It has been shown [3, 4, 6] that for any energy belonging to the continues spectra, $E_n \in E_c$, the corresponding asymptotic eigenstate $\psi_{n,\beta}^R$ satisfying

$$H_{\text{spinless}}\psi_{n,\beta}^R = E_n\psi_{n,\beta}^R \quad (84)$$

is the superposition of two non-Bloch waves,

$$\psi_{n,\beta}^R = c_{n,2}\psi_{n,\beta}^R(\beta_{n,2}) + c_{n,3}\psi_{n,\beta}^R(\beta_{n,3}) \quad (85)$$

where $\beta_{n,2/3}$ are the solutions of

$$f(\beta, E_n) = \det[E_n - \mathcal{H}_{\text{spinless}}(\beta)] = 0 \quad (86)$$

with the following orders

$$|\beta_{n,1}| \leq |\beta_{n,2}| \leq |\beta_{n,3}| \leq |\beta_{n,4}|. \quad (87)$$

Here the non-Bloch wave has the following form in real space,

$$\psi_{n,\beta}^R(\beta_{n,i}) = u_{\mu_{n,i}}^R(\beta_{n,i}) \otimes \phi(\beta_{n,i}), \quad (88)$$

where

$$\phi(\beta_{n,i}) = (\beta_{n,i}, \beta_{n,i}^2, \dots, \beta_{n,i}^{N-1}, \beta_{n,i}^N)^t, \quad (89)$$

and $u_{\mu_{n,i}}^R(\beta_{n,i})$ is the $\mu_{n,i}$ -th eigenstate of $\mathcal{H}_{\text{spinless}}(\beta_{n,i})$ with energy $E_{\mu_{n,i}}(\beta_{n,i}) = E_n$. Since $\beta_{n,i} = r_n e^{ik_{n,i}}$, $\phi(\beta_{n,i})$ can be expressed as

$$\phi(\beta_{n,i}) = (r_n e^{ik_{n,i}}, r_n^2 e^{2ik_{n,i}}, \dots, r_n^{N-1} e^{i(N-1)k_{n,i}}, r_n^N e^{iNk_{n,i}})^t = U(r_n)\phi(k_{n,i}), \quad (90)$$

where $U(r_n) = \text{diag}[r_n, \dots, r_n^N]$, and $\phi(k_{n,i}) = (e^{ik_{n,i}}, e^{2ik_{n,i}}, \dots, e^{i(N-1)k_{n,i}}, e^{iNk_{n,i}})^t$.

In summary, we have

$$\begin{aligned} H_{\text{spinless}}\psi_{n,\beta}^R &= E_n\psi_{n,\beta}^R, & \psi_{n,\beta}^R &= c_{n,2}\psi_{n,\beta}^R(\beta_{n,2}) + c_{n,3}\psi_{n,\beta}^R(\beta_{n,3}) \\ & & &= U(r_n)(c_{n,2}\psi_{n,k}^R(k_{n,2}) + c_{n,3}\psi_{n,k}^R(k_{n,2})) \\ & & &= U(r_n)\psi_{n,k}^R. \end{aligned} \quad (91)$$

where $\psi_{n,k}^R(k_{n,i}) = u_{\mu_{n,i}}^R(\beta_{n,i}) \otimes \phi(k_{n,i})$, which is a conventional Bloch wave.

3. Left eigenstate of the open boundary Hamiltonian

The Hermitian conjugate of H_{spinless} is

$$H_{\text{spinless}}^\dagger = \begin{pmatrix} -i\gamma + \mu & t_1 & i\lambda & 0 & \dots & 0 & 0 & 0 & 0 \\ t_1 & i\gamma - \mu & t_2 & -i\lambda & \dots & 0 & 0 & 0 & 0 \\ -i\lambda & t_2 & -i\gamma + \mu & t_1 & \dots & 0 & 0 & 0 & 0 \\ 0 & i\lambda & t_1 & i\gamma - \mu & \dots & 0 & 0 & 0 & 0 \\ \dots & \dots \\ 0 & 0 & 0 & 0 & \dots & -i\gamma + \mu & t_1 & -i\lambda & 0 \\ 0 & 0 & 0 & 0 & \dots & t_1 & i\gamma - \mu & t_2 & i\lambda \\ 0 & 0 & 0 & 0 & \dots & i\lambda & t_2 & -i\gamma + \mu & t_1 \\ 0 & 0 & 0 & 0 & \dots & 0 & -i\lambda & t_1 & i\gamma - \mu \end{pmatrix} \quad (92)$$

The corresponding bulk Hamiltonian becomes

$$[\mathcal{H}(1/\beta^*)]^\dagger \quad (93)$$

To show this, we can expand the Hamiltonian in the form of creation and annihilation operators:

$$H = \sum_{i,j} \sum_{\mu,\nu} t_{ij}^{\mu\nu} \hat{c}_{i\mu}^\dagger \hat{c}_{j\nu} \rightarrow \sum_{l=-l_1}^{l_2} t_{ij}^{\mu\nu} \delta_{i+l,j} e^{ikl} \rightarrow \sum_{l=-l_1}^{l_2} t_{ij}^{\mu\nu} \delta_{i+l,j} \beta^l \rightarrow \mathcal{H}(\beta) \quad (94)$$

consequently, we obtain

$$\begin{aligned} H^\dagger &= \sum_{i,j} \sum_{\mu,\nu} (t_{ji}^{\nu\mu})^* \hat{c}_{i\mu}^\dagger \hat{c}_{j\nu} \rightarrow \sum_{l=-l_1}^{l_2} (t_{ji}^{\nu\mu})^* \delta_{i+l,j} e^{ikl} \rightarrow \sum_{l=-l_1}^{l_2} (t_{ji}^{\nu\mu})^* \delta_{i+l,j} \beta^l \\ &= \left[\sum_{l=-l_1}^{l_2} t_{ij}^{\mu\nu} \delta_{i+l,j} (\beta^*)^{-l} \right]^\dagger \\ &= [\mathcal{H}(1/\beta^*)]^\dagger \end{aligned} \quad (95)$$

Therefore, according to the GBZ condition, we know the left eigenstate satisfying

$$H_{\text{spinless}}^\dagger \psi_{n,\beta}^L = E_n^* \psi_{n,\beta}^L \quad (96)$$

can be expressed as

$$\begin{aligned} \psi_{n,\beta}^L &= d_{n,2} \psi_{n,\beta}^L(1/\beta_{n,2}^*) + d_{n,3} \psi_{n,\beta}^L(1/\beta_{n,3}^*) \\ &= U(1/r_n) (d_{n,2} \psi_{n,k}^L(k_{n,2}) + d_{n,3} \psi_{n,k}^L(k_{n,2})) \\ &= U(1/r_n) \psi_{n,k}^L \end{aligned} \quad (97)$$

where $\psi_{n,k}^L(k_{n,i}) = u_{\mu_n,i}^L(1/\beta_{n,i}^*) \otimes \phi(k_{n,i})$, which is also a conventional Bloch wave. The normalization condition requires

$$\langle \psi_{n,\beta}^L | \psi_{n,\beta}^R \rangle = \langle \psi_{n,k}^L | \psi_{n,k}^R \rangle = 1 \quad (98)$$

C. Local density of states

The local DoS with open boundary condition at site i is defined as

$$\nu_i(\omega) = -\frac{1}{\pi} \text{Im}[\langle i | G^R(\omega) | i \rangle] = -\frac{1}{\pi} \text{Im} \left[\sum_n \frac{\langle i | \psi_{n,\beta}^R \rangle \langle \psi_{n,\beta}^L | i \rangle}{\omega - E_n} \right] = -\frac{1}{\pi} \text{Im} \left[\sum_n \frac{\langle i | \psi_{n,k}^R \rangle \langle \psi_{n,k}^L | i \rangle}{\omega - E_n} \right], \quad (99)$$

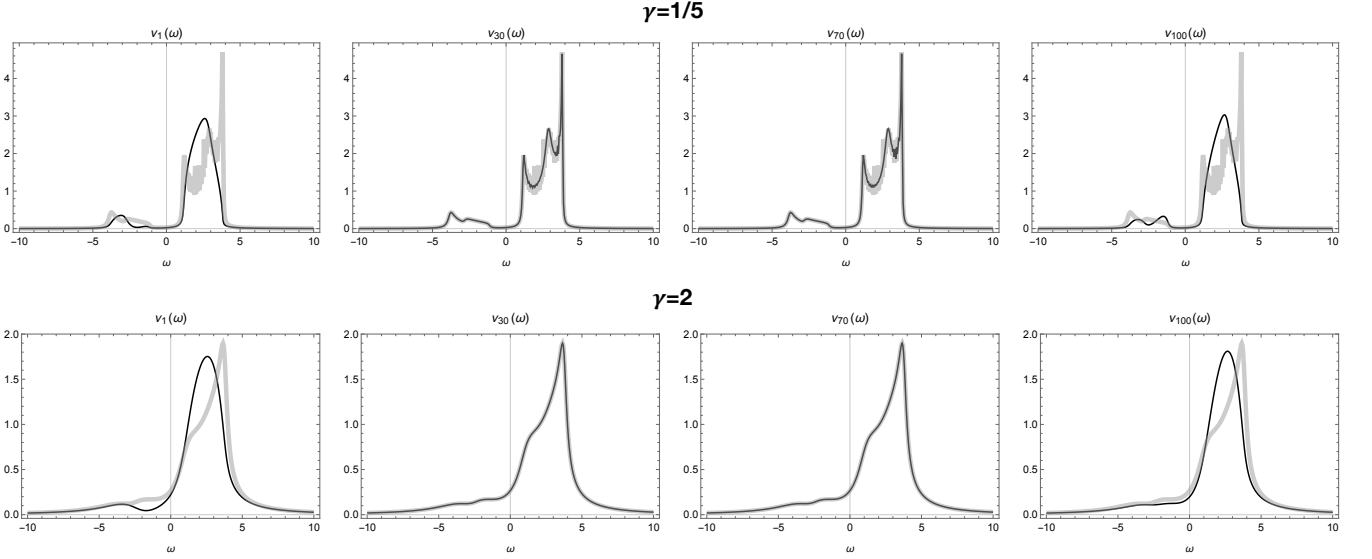


FIG. 4. The local DoS of the spinless model $H_{\text{spinless}} - i\gamma$ with $t_1 = 2, t_2 = \mu = \lambda = 1$ and different values of γ . The gray/black lines represent local DoS with periodic/open boundaries. One can notice the similar behavior of local DoS at the left/right ends of the lattice, although the system has skin modes localized at the left end of the lattice (see Fig. 1 in the main text).

where we used $\langle i|\psi_{n,\beta}^R\rangle = \langle i|U(r_n)|\psi_{n,k}^R\rangle = r_n^i \langle i|\psi_{n,k}^R\rangle$. The above formula shows that the local DoS does not depend on the localization length of skin modes, namely, r_n . In Fig. 4, we show the comparison between the open/periodic boundary local DoS. The model Hamiltonian is $H_{\text{spinless}} - i\gamma$ with $t_1 = 2, t_2 = \mu = \lambda = 1$ and different values of γ . The gray/black lines represent local DoS with periodic/open boundaries. One can notice the similar behavior of local DoS at the left/right ends of the lattice, although the system has skin modes localized at the left end of the lattice (see Fig. 1 in the main text).

D. Tunneling probability

In the main text, we have shown that the propagator from site i to site f can be expressed as

$$\langle f|U(t)|i\rangle = \sum_n r_n^{f-i} e^{-iE_n t} \langle f|\psi_{n,k}^R\rangle \langle \psi_{n,k}^L|i\rangle, \quad (100)$$

where r_n represents the localization length of the skin modes. When $r_n < 1$, it seems that the term r_n^{1-N} will tend to infinity in the limit of $N \rightarrow \infty$. Now we show that in spite of the existence of a seemingly divergent term r_n^{f-i} , the tunneling probability

$$P_{f \leftarrow i}(t) = |\langle f|U(t)|i\rangle|^2 \quad (101)$$

is bounded to less than 1, when the system is purely dissipative.

First, we notice that

$$\langle i|U^\dagger(t)U(t)|i\rangle = \sum_f |G_{f \leftarrow i}(t)|^2 = \sum_f P_{f \leftarrow i}(t). \quad (102)$$

If we take $t = 0$ in the above equation, we can obtain $\langle i|U^\dagger(t)U(t)|i\rangle = \sum_f |G_{f \leftarrow i}(t)|^2 = 1$, which means $P_{f \leftarrow i}(t = 0) = |G_{f \leftarrow i}(t = 0)|^2 \leq 1$. On the other hand, if we plug in the expansion of the time evolution operator $U(t)$, we have

$$\langle i|U^\dagger(t)U(t)|i\rangle = \sum_{mn} \langle i|\psi_m^L\rangle \langle \psi_m^R|\psi_n^R\rangle \langle \psi_n^L|i\rangle e^{i(E_m^* - E_n)t} \equiv \sum_{mn} T_{mn}, \quad (103)$$

where

$$T_{mn} = \langle i|\psi_m^L\rangle \langle \psi_m^R|\psi_n^R\rangle \langle \psi_n^L|i\rangle e^{i(E_m^* - E_n)t} \quad (104)$$

and $|\psi_m^{R/L}\rangle$ represent the right/left eigenstate, which can be skin modes or non-skin modes.

If we take $m = n$, we will have

$$T_{nn} = \langle i|\psi_n^L\rangle\langle\psi_n^R|\psi_n^R\rangle\langle\psi_n^L|i\rangle e^{i(E_n^* - E_n)t}. \quad (105)$$

Since the system is dissipative, the imaginary part of the eigenvalue must be negative. Thus without loss of generality, we can write $E_n = a_n - ib_n$ with $b_n > 0$ (dissipation), then

$$T_{nn} = \langle i|\psi_n^L\rangle\langle\psi_n^R|\psi_n^R\rangle\langle\psi_n^L|i\rangle e^{-2b_n t}, \quad (106)$$

which will decay with time.

On the other hand, if $m \neq n$, then

$$T_{mn} + T_{nm} = c_{mn} e^{i(E_m^* - E_n)t} + c_{mn}^* e^{i(E_n^* - E_m)t} \propto e^{-b_{mn}t}, \quad (107)$$

where

$$b_{mn} = \text{Im}[E_m^* - E_n] = b_m + b_n, \quad (108)$$

which will also decay with time.

Therefore, we finally obtain that $\langle i|U^\dagger(t)U(t)|i\rangle$ will decay with time, which gives the upper bounds of $P_{f\leftarrow i}(t)$

$$P_{f\leftarrow i}(t) = \sum_f P_{f\leftarrow i}(t) = \langle i|U^\dagger(t)U(t)|i\rangle \leq \langle i|U^\dagger(0)U(0)|i\rangle = 1. \quad (109)$$

V. MATHEMATICA CODE

In the following pages, we provide a Mathematica code to calculate the auxiliary GBZ [3] of the spinful model proposed in the main text.

-
- [1] C.-K. Chiu, J. C. Y. Teo, A. P. Schnyder, and S. Ryu, *Rev. Mod. Phys.* **88**, 035005 (2016).
 - [2] K. Kawabata, K. Shiozaki, M. Ueda, and M. Sato, *Phys. Rev. X* **9**, 041015 (2019).
 - [3] Z. Yang, K. Zhang, C. Fang, and J. Hu, arXiv e-prints, arXiv:1912.05499 (2019), [arXiv:1912.05499 \[cond-mat.mes-hall\]](#).
 - [4] K. Zhang, Z. Yang, and C. Fang, [arXiv:1910.01131](#).
 - [5] N. Okuma, K. Kawabata, K. Shiozaki, and M. Sato, [arXiv:1910.02878](#).
 - [6] K. Yokomizo and S. Murakami, *Phys. Rev. Lett.* **123**, 066404 (2019).

The Bloch Hamiltonian

```

In[ ]:= Hk[k_, t1_, t2_, λI_, λR_, μ_, γ_] := (t1 + t2 Cos[k]) ArrayFlatten[TensorProduct[{{0, 1}, {1, 0}}, {{1, 0}, {0, 1}}]] +
t2 Sin[k] ArrayFlatten[TensorProduct[{{0, -I}, {I, 0}}, {{1, 0}, {0, 1}}]] +
μ ArrayFlatten[TensorProduct[{{1, 0}, {0, -1}}, {{1, 0}, {0, 1}}]] +
λI Sin[k] ArrayFlatten[TensorProduct[{{1, 0}, {0, -1}}, {{1, 0}, {0, -1}}]] -
λR (1/2 ArrayFlatten[TensorProduct[{{0, -I}, {I, 0}}, {{0, 1}, {1, 0}}]] -
3^(1/2)/2 ArrayFlatten[TensorProduct[{{0, -I}, {I, 0}}, {{0, -I}, {I, 0}}]]) +
I γ ArrayFlatten[TensorProduct[{{1, 0}, {0, -1}}, {{1, 0}, {0, 1}}]];
Hk[k, t1, t2, λI, λR, μ, γ] // MatrixForm

```

Out[]/MatrixForm=

$$\begin{pmatrix}
 i\gamma + \mu + \lambda I \sin[k] & 0 & t1 + t2 \cos[k] - i t2 \sin[k] & -\left(-\frac{i}{2} + \frac{\sqrt{3}}{2}\right) \lambda R \\
 0 & i\gamma + \mu - \lambda I \sin[k] & -\left(-\frac{i}{2} - \frac{\sqrt{3}}{2}\right) \lambda R & t1 + t2 \cos[k] - i t2 \sin[k] \\
 t1 + t2 \cos[k] + i t2 \sin[k] & -\left(\frac{i}{2} - \frac{\sqrt{3}}{2}\right) \lambda R & -i\gamma - \mu - \lambda I \sin[k] & 0 \\
 -\left(\frac{i}{2} + \frac{\sqrt{3}}{2}\right) \lambda R & t1 + t2 \cos[k] + i t2 \sin[k] & 0 & -i\gamma - \mu + \lambda I \sin[k]
 \end{pmatrix}$$

The real space Hamiltonian

```

In[ ]:= Hr[t1_, t2_, λI_, λR_, μ_, γ_, n_] :=
SparseArray[Band[{1, 1}, {n, n}] → {Coefficient[TrigToExp[Hk[k, t1, t2, λI, λR, μ, γ]], Exp[I k], 0]}, {n, n}] +
SparseArray[Band[{5, 1}, {n, n}] → {Coefficient[TrigToExp[Hk[k, t1, t2, λI, λR, μ, γ]], Exp[I k], -1]}, {n, n}] +
SparseArray[Band[{1, 5}, {n, n}] → {Coefficient[TrigToExp[Hk[k, t1, t2, λI, λR, μ, γ]], Exp[I k], 1]}, {n, n}];

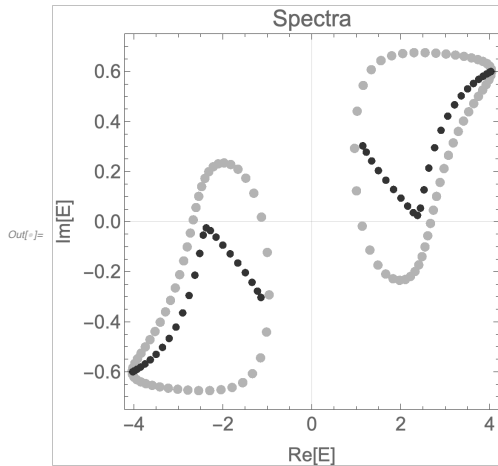
```

Periodic/open boundary spectra

```

In[ ]:= PeriodicSpectra = Flatten[Table[Eigenvalues[N[Hk[k, 2, 1, 2, 1, 1, 1]]], {k, -3.14, 3.14, 3.14/25}], 1];
(*N=100/4=25*) OpenSpectra = Eigenvalues[N[Hr[2, 1, 2, 1, 1, 1, 100], 50]];
Spectra = ListPlot[({Tooltip[Re[#1], Im[#1]] & }/@PeriodicSpectra, (Tooltip[Re[#1], Im[#1]] & )/@OpenSpectra),
PlotTheme → "Scientific", AspectRatio → 1, PlotRange → All,
PlotStyle → {{GrayLevel[0.7], PointSize[0.025]}, {GrayLevel[0.2], PointSize[0.02]}}, {GrayLevel[0.1], PointSize[0.01]}},
ImageSize → 350, FrameLabel → {{HoldForm["Im[E]"], None}, {HoldForm["Re[E]"], None}},
PlotLabel → HoldForm[Spectra], LabelStyle → {GrayLevel[0.4], 15}]

```



Non-Bloch Hamiltonian and its characteristic equation

```

In[ ]:= Hb[β_, t1_, t2_, λI_, λR_, μ_, γ_] := TrigToExp[Hk[k, t1, t2, λI, λR, μ, γ]] /. {Exp[I k] → β, Exp[-I k] → 1/β}
Hb[β, t1, t2, λI, λR, μ, γ] // MatrixForm
F[β_, Ene_, t1_, t2_, λI_, λR_, μ_, γ_] := Factor[Det[Ene IdentityMatrix[4] - Hb[β, t1, t2, λI, λR, μ, γ]]];

```

Out[]/MatrixForm=

$$\begin{pmatrix}
 i\gamma + \frac{i\lambda I}{2\beta} - \frac{i\beta\lambda I}{2} + \mu & 0 & t1 + \frac{t2}{\beta} & \frac{i\lambda R}{2} - \frac{\sqrt{3}\lambda R}{2} \\
 0 & i\gamma - \frac{i\lambda I}{2\beta} + \frac{i\beta\lambda I}{2} + \mu & \frac{i\lambda R}{2} + \frac{\sqrt{3}\lambda R}{2} & t1 + \frac{t2}{\beta} \\
 t1 + t2\beta & -\frac{i\lambda R}{2} + \frac{\sqrt{3}\lambda R}{2} & -i\gamma - \frac{i\lambda I}{2\beta} + \frac{i\beta\lambda I}{2} - \mu & 0 \\
 -\frac{i\lambda R}{2} - \frac{\sqrt{3}\lambda R}{2} & t1 + t2\beta & 0 & -i\gamma + \frac{i\lambda I}{2\beta} - \frac{i\beta\lambda I}{2} - \mu
 \end{pmatrix}$$

Auxiliary GBZ (arXiv:1912.05499)

1. Eliminating E

```

In[ ]:= Res[β1_, β2_, t_, t1_, t2_, λI_, λR_, μ_, γ_] :=
  Resultant[F[β1 + I β2, Ene, t1, t2, λI, λR, μ, γ], F[(β1 + I β2) ((1 - t^2 + 2 I t) / (1 + t^2)), Ene, t1, t2, λI, λR, μ, γ], Ene];
g0 = FactorList[Factor[Res[β1, β2, t, 2, 1, 2, 1, 1, 1] ((-i + t)^16 (i + t)^16 (β1 + i β2)^16) / (256 t^4)]]

Out[ ]:= {{1, 1}, {i + t - i β1^2 + t β1^2 + 2 β1 β2 + 2 i t β1 β2 + i β2^2 - t β2^2, 4},
  {4 t^2 - 8 i t^3 - 4 t^4 - 8 t^2 β1 + 8 i t^3 β1 - 8 t^4 β1 + 8 i t^5 β1 - (5 + 8 i) β1^2 + (2 - 16 i) t^2 β1^2 + (11 - 8 i) t^4 β1^2 +
  4 t^6 β1^2 - 8 t^2 β1^3 - 8 i t^3 β1^3 - 8 t^4 β1^3 - 8 i t^5 β1^3 + 4 t^2 β1^4 + 8 i t^3 β1^4 - 4 t^4 β1^4 - 8 i t^2 β2 - 8 t^3 β2 - 8 i t^4 β2 - 8 t^5 β2 +
  (16 - 10 i) β1 β2 + (32 + 4 i) t^2 β1 β2 + (16 + 22 i) t^4 β1 β2 + 8 i t^6 β1 β2 - 24 i t^2 β1^2 β2 + 24 t^3 β1^2 β2 - 24 i t^4 β1^2 β2 +
  24 t^5 β1^2 β2 + 16 i t^2 β1^3 β2 - 32 t^3 β1^3 β2 - 16 i t^4 β1^3 β2 + (5 + 8 i) β2^2 - (2 - 16 i) t^2 β2^2 - (11 - 8 i) t^4 β2^2 - 4 t^6 β2^2 +
  24 t^2 β1 β2^2 + 24 i t^3 β1 β2^2 + 24 t^4 β1 β2^2 + 24 i t^5 β1 β2^2 - 24 t^2 β1^2 β2^2 - 48 i t^3 β1^2 β2^2 + 24 t^4 β1^2 β2^2 + 8 i t^2 β2^3 -
  8 t^3 β2^3 + 8 i t^4 β2^3 - 8 t^5 β2^3 - 16 i t^2 β1 β2^3 + 32 t^3 β1 β2^3 + 16 i t^4 β1 β2^3 + 4 t^2 β2^4 + 8 i t^3 β2^4 - 4 t^4 β2^4, 2},
  {-4 + 16 i t + 24 t^2 - 16 i t^3 - 4 t^4 + 8 β1 - 24 i t β1 - 16 t^2 β1 - 16 i t^3 β1 - 24 t^4 β1 + 8 i t^5 β1 - (9 + 8 i) β1^2 - (16 - 18 i) t β1^2 -
  (9 + 8 i) t^2 β1^2 - (32 - 36 i) t^3 β1^2 + (9 + 8 i) t^4 β1^2 - (16 - 18 i) t^5 β1^2 + (9 + 8 i) t^6 β1^2 - 8 β1^3 + 8 i t β1^3 - 16 t^2 β1^3 + 16 i t^3 β1^3 -
  8 t^4 β1^3 + 8 i t^5 β1^3 + (6 - 16 i) β1^4 + (10 - 48 i) t^2 β1^4 + (2 - 48 i) t^4 β1^4 - (2 + 16 i) t^6 β1^4 - 8 β1^5 - 8 i t β1^5 - 16 t^2 β1^5 - 16 i t^3 β1^5 -
  8 t^4 β1^5 - 8 i t^5 β1^5 + (16 - 18 i) t β1^6 - (9 + 8 i) t^2 β1^6 + (32 - 36 i) t^3 β1^6 + (9 + 8 i) t^4 β1^6 + (16 - 18 i) t^5 β1^6 +
  (9 + 8 i) t^6 β1^6 + 8 β1^7 + 24 i t β1^7 - 16 t^2 β1^7 + 16 i t^3 β1^7 - 24 t^4 β1^7 - 8 i t^5 β1^7 - 4 β1^8 - 16 i t β1^8 + 24 t^2 β1^8 + 16 i t^3 β1^8 -
  4 t^4 β1^8 + 8 i β2 + 24 t β2 - 16 i t^2 β2 + 16 t^3 β2 - 24 i t^4 β2 - 8 t^5 β2 + (16 - 18 i) β1 β2 - (36 + 32 i) t β1 β2 + (16 - 18 i) t^2 β1 β2 -
  (72 + 64 i) t^3 β1 β2 - (16 - 18 i) t^4 β1 β2 - (36 + 32 i) t^5 β1 β2 - (16 - 18 i) t^6 β1 β2 - 24 i β1^2 β2 - 24 t β1^2 β2 - 48 i t^2 β1^2 β2 -
  48 t^3 β1^2 β2 - 24 i t^4 β1^2 β2 - 24 t^5 β1^2 β2 + (64 + 24 i) β1^3 β2 + (192 + 40 i) t^2 β1^3 β2 + (192 + 8 i) t^4 β1^3 β2 + (64 - 8 i) t^6 β1^3 β2 -
  40 i β1^4 β2 + 40 t β1^4 β2 - 80 i t^2 β1^4 β2 + 80 t^3 β1^4 β2 - 40 i t^4 β1^4 β2 + 40 t^5 β1^4 β2 + (48 - 54 i) β1^5 β2 + (108 + 96 i) t β1^5 β2 +
  (48 - 54 i) t^2 β1^5 β2 + (216 + 192 i) t^3 β1^5 β2 - (48 - 54 i) t^4 β1^5 β2 + (108 + 96 i) t^5 β1^5 β2 - (48 - 54 i) t^6 β1^5 β2 -
  168 t β1^6 β2 - 112 i t^2 β1^6 β2 - 112 t^3 β1^6 β2 - 168 i t^4 β1^6 β2 + 56 t^5 β1^6 β2 - 32 i β1^7 β2 + 128 t β1^7 β2 + 192 i t^2 β1^7 β2 - 128 t^3 β1^7 β2 -
  32 i t^4 β1^7 β2 + (9 + 8 i) β2^2 + (16 - 18 i) t β2^2 + (9 + 8 i) t^2 β2^2 + (32 - 36 i) t^3 β2^2 - (9 + 8 i) t^4 β2^2 + (16 - 18 i) t^5 β2^2 - (9 + 8 i) t^6 β2^2 +
  24 β1 β2^2 - 24 i t β1 β2^2 + 48 t^2 β1 β2^2 - 48 i t^3 β1 β2^2 + 24 t^4 β1 β2^2 - 24 i t^5 β1 β2^2 - (36 - 96 i) β1^2 β2^2 - (60 - 288 i) t^2 β1^2 β2^2 -
  (12 - 288 i) t^4 β1^2 β2^2 + (12 + 96 i) t^6 β1^2 β2^2 + 80 β1^3 β2^2 + 80 i t β1^3 β2^2 + 160 t^2 β1^3 β2^2 + 160 i t^3 β1^3 β2^2 + 80 t^4 β1^3 β2^2 + 80 i t^5 β1^3 β2^2 +
  (135 + 120 i) β1^4 β2^2 - (240 - 270 i) t β1^4 β2^2 + (135 + 120 i) t^2 β1^4 β2^2 - (480 - 540 i) t^3 β1^4 β2^2 - (135 - 120 i) t^4 β1^4 β2^2 -
  (240 - 270 i) t^5 β1^4 β2^2 - (135 + 120 i) t^6 β1^4 β2^2 - 168 β1^5 β2^2 - 504 i t β1^5 β2^2 + 336 t^2 β1^5 β2^2 - 336 i t^3 β1^5 β2^2 + 504 t^4 β1^5 β2^2 +
  168 i t^5 β1^5 β2^2 + 112 β1^6 β2^2 + 448 i t β1^6 β2^2 - 672 t^2 β1^6 β2^2 - 448 i t^3 β1^6 β2^2 + 112 t^4 β1^6 β2^2 + 8 i β2^3 + 8 t β2^3 + 16 i t^2 β2^3 +
  16 t^3 β2^3 + 8 i t^4 β2^3 + 8 t^5 β2^3 - (64 + 24 i) β1 β2^3 - (192 + 40 i) t β1 β2^3 - (192 + 8 i) t^2 β1 β2^3 - (64 - 8 i) t^4 β1 β2^3 + 80 i β1^2 β2^3 -
  80 t β1^2 β2^3 + 160 i t^2 β1^2 β2^3 - 160 t^3 β1^2 β2^3 + 80 i t^4 β1^2 β2^3 - 80 t^5 β1^2 β2^3 - (160 - 180 i) β1^3 β2^3 - (360 + 320 i) t β1^3 β2^3 -
  (160 - 180 i) t^2 β1^3 β2^3 - (720 + 640 i) t^3 β1^3 β2^3 + (160 - 180 i) t^4 β1^3 β2^3 - (360 + 320 i) t^5 β1^3 β2^3 + (160 - 180 i) t^6 β1^3 β2^3 -
  280 i β1^4 β2^3 + 840 t β1^4 β2^3 + 560 i t^2 β1^4 β2^3 + 560 t^3 β1^4 β2^3 + 840 i t^4 β1^4 β2^3 - 280 t^5 β1^4 β2^3 + 224 i β1^5 β2^3 - 896 t β1^5 β2^3 -
  1344 i t^2 β1^5 β2^3 + 896 t^3 β1^5 β2^3 + 224 i t^4 β1^5 β2^3 + (6 - 16 i) β2^4 + (10 - 48 i) t^2 β2^4 + (2 - 48 i) t^4 β2^4 - (2 + 16 i) t^6 β2^4 -
  40 β1 β2^4 - 40 i t β1 β2^4 - 80 t^2 β1 β2^4 - 80 i t^3 β1 β2^4 - 40 t^4 β1 β2^4 - 40 i t^5 β1 β2^4 - (135 + 120 i) β1^2 β2^4 + (240 - 270 i) t β1^2 β2^4 -
  (135 + 120 i) t^2 β1^2 β2^4 + (480 - 540 i) t^3 β1^2 β2^4 + (135 + 120 i) t^4 β1^2 β2^4 + (240 - 270 i) t^5 β1^2 β2^4 + (135 + 120 i) t^6 β1^2 β2^4 +
  280 β1^3 β2^4 + 840 i t β1^3 β2^4 - 560 t^2 β1^3 β2^4 + 560 i t^3 β1^3 β2^4 - 840 t^4 β1^3 β2^4 - 280 i t^5 β1^3 β2^4 - 280 β1^4 β2^4 - 1120 i t β1^4 β2^4 +
  1680 t^2 β1^4 β2^4 + 1120 i t^3 β1^4 β2^4 - 280 t^4 β1^4 β2^4 - 8 i β2^5 + 8 t β2^5 - 16 i t^2 β2^5 + 16 t^3 β2^5 - 8 i t^4 β2^5 + 8 t^5 β2^5 + (48 - 54 i) β1 β2^5 +
  (108 + 96 i) t β1 β2^5 + (48 - 54 i) t^2 β1 β2^5 + (216 + 192 i) t^3 β1 β2^5 - (48 - 54 i) t^4 β1 β2^5 + (108 + 96 i) t^5 β1 β2^5 - (48 - 54 i) t^6 β1 β2^5 +
  168 i β1^2 β2^5 - 504 t β1^2 β2^5 - 336 i t^2 β1^2 β2^5 - 336 t^3 β1^2 β2^5 - 504 i t^4 β1^2 β2^5 + 168 t^5 β1^2 β2^5 - 224 i β1^3 β2^5 + 896 t β1^3 β2^5 +
  1344 i t^2 β1^3 β2^5 - 896 t^3 β1^3 β2^5 - 224 i t^4 β1^3 β2^5 + (9 + 8 i) β2^6 - (16 - 18 i) t β2^6 + (9 + 8 i) t^2 β2^6 - (32 - 36 i) t^3 β2^6 - (9 + 8 i) t^4 β2^6 -
  (16 - 18 i) t^5 β2^6 - (9 + 8 i) t^6 β2^6 - 56 β1 β2^6 - 168 i t β1 β2^6 + 112 t^2 β1 β2^6 - 112 i t^3 β1 β2^6 + 168 t^4 β1 β2^6 + 56 i t^5 β1 β2^6 + 112 β1^2 β2^6 +
  448 i t β1^2 β2^6 - 672 t^2 β1^2 β2^6 - 448 i t^3 β1^2 β2^6 + 112 t^4 β1^2 β2^6 - 8 i β2^7 + 24 t β2^7 + 16 i t^2 β2^7 + 16 t^3 β2^7 + 24 i t^4 β2^7 - 8 t^5 β2^7 +
  32 i β1 β2^7 - 128 t β1 β2^7 - 192 i t^2 β1 β2^7 + 128 t^3 β1 β2^7 + 32 i t^4 β1 β2^7 - 4 β2^8 - 16 i t β2^8 + 24 t^2 β2^8 + 16 i t^3 β2^8 - 4 t^4 β2^8, 2}}

```

2. Eliminating t for each factor

```

In[ ]:= g1a = ComplexExpand[Re[g0[[2]][[1]]]];
g1b = ComplexExpand[Im[g0[[2]][[1]]]];
aGBZ1 = Resultant[g1a, g1b, t];

In[ ]:= g2a = ComplexExpand[Re[g0[[3]][[1]]]];
g2b = ComplexExpand[Im[g0[[3]][[1]]]];
aGBZ2 = Factor[Resultant[g2a, g2b, t]];

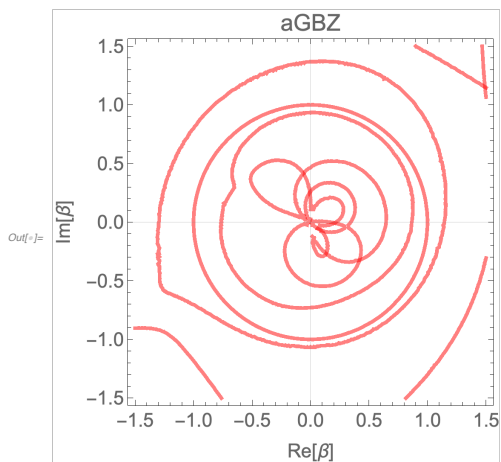
In[ ]:= g3a = ComplexExpand[Re[g0[[4]][[1]]]];
g3b = ComplexExpand[Im[g0[[4]][[1]]]];
aGBZ3 = Factor[Resultant[g3a, g3b, t]];

```

```

In[ ]:= aGBZ = ContourPlot[{aGBZ1 == 0, aGBZ2 == 0, aGBZ3 == 0}, {β1, -1.5, 1.5}, {β2, -1.5, 1.5},
  PlotTheme -> "Scientific", ImageSize -> 350, ContourStyle -> {{RGBColor[1, 0, 0.5], Thickness[0.01]},
  {RGBColor[1, 0, 0.5], Thickness[0.01]}, {RGBColor[1, 0, 0.5], Thickness[0.01]}},
  FrameLabel -> {{HoldForm["Im[β]"], None}, {HoldForm["Re[β]"], None}}, PlotLabel -> HoldForm[aGBZ],
  LabelStyle -> {GrayLevel[0.4], 15}]

```



GBZ

```

In[ ]:= GBZ1 = Table[Sort[z /. NSolve[F[z, OpenSpectra[[i]], 2, 1, 2, 1, 1, 1], z], Abs[#1] < Abs[#2] &][[3]], {i, 1, 100}];
GBZ2 = Table[Sort[z /. NSolve[F[z, OpenSpectra[[i]], 2, 1, 2, 1, 1, 1], z], Abs[#1] < Abs[#2] &][[4]], {i, 1, 100}];
GBZ3 = Table[Sort[z /. NSolve[F[z, OpenSpectra[[i]], 2, 1, 2, 1, 1, 1], z], Abs[#1] < Abs[#2] &][[5]], {i, 1, 100}];
GBZ4 = Table[Sort[z /. NSolve[F[z, OpenSpectra[[i]], 2, 1, 2, 1, 1, 1], z], Abs[#1] < Abs[#2] &][[6]], {i, 1, 100}];

In[ ]:= Show[{aGBZ, Graphics[{Table[{Black, Opacity[0.8], PointSize[0.02], Point[{Re[GBZ1[[i]]], Im[GBZ1[[i]]}]}], {i, 1, 100}},
  Table[{Black, Opacity[0.8], PointSize[0.02], Point[{Re[GBZ2[[i]]], Im[GBZ2[[i]]}]}], {i, 1, 100}},
  Table[{Black, Opacity[0.8], PointSize[0.02], Point[{Re[GBZ3[[i]]], Im[GBZ3[[i]]}]}], {i, 1, 100}},
  Table[{Black, Opacity[0.8], PointSize[0.02], Point[{Re[GBZ4[[i]]], Im[GBZ4[[i]]}]}], {i, 1, 100}}]}]}

```

